Ultrasound in Med. & Biol., Vol. 00, No. 00, pp. 1–23, 2019

0301-5629/$ - see front matter

https://doi.org/10.1016/j.ultrasmedbio.2019.09.011

● *Review Article*

SONOBACTERICIDE: AN EMERGING TREATMENT STRATEGY FOR BACTERIAL INFECTIONS

KIRBY R. LATTWEIN,* HIMANSHU SHEKHAR,† JOOP J.P. KOUIJZER,* WILLEM J.B. VAN WAMEL,‡ CHRISTY K. HOLLAND,† and KLAZINA KOOIMAN*

* Department of Biomedical Engineering, Thoraxcenter, Erasmus MC, University Medical Center Rotterdam, Rotterdam, The Netherlands; † Division of Cardiovascular Health and Disease, Department of Internal Medicine, University of Cincinnati, Cincinnati, Ohio, USA; and ‡ Department of Medical Microbiology and Infectious Diseases, Erasmus MC, University Medical Center Rotterdam, Rotterdam, The Netherlands

(*Received* 17 *April* 2019; *revised* 3 *September* 2019; *in final from* 16 *September* 2019)

Abstract—Ultrasound has been developed as both a diagnostic tool and a potent promoter of beneficial bio-effects for the treatment of chronic bacterial infections. Bacterial infections, especially those involving biofilm on implants, indwelling catheters and heart valves, affect millions of people each year, and many deaths occur as a consequence. Exposure of microbubbles or droplets to ultrasound can directly affect bacteria and enhance the efficacy of antibiotics or other therapeutics, which we have termed *sonobactericide*. This review summarizes investigations that have provided evidence for ultrasound-activated microbubble or droplet treatment of bacteria and biofilm. In particular, we review the types of bacteria and therapeutics used for treatment and the *in vitro* and pre-clinical experimental setups employed in sonobactericide research. Mechanisms for ultrasound enhancement of sonobactericide, with a special emphasis on acoustic cavitation and radiation force, are reviewed, and the potential for clinical translation is discussed. (E-mail: k.lattwein@erasmusmc.nl) © 2019 The Author(s). Published by Elsevier Inc. on behalf of World Federation for Ultrasound in Medicine & Biology. This is an open access article under the CC BY-NC-ND license. (http://creativecommons.org/licenses/by-nc-nd/4.0/).

Key Words: **Antibiotic, Bacteria, Biofilm, Contrast agents, Infection, Microbubbles, Nanodroplet, Sonobactericide, Ultrasound.**

INTRODUCTION

In recent decades, the combination of ultrasound and cavitation nuclei has been investigated as an alternative approach to treatment of several life-threatening diseases. Ultrasound is a common diagnostic tool and offers several advantages: it is non-invasive and inexpensive, available at the point-of-care, and is a safe medical application. Many different types of cavitation nuclei exist, including gas or liquid filled and coated or non-coated. These include micro- and nanobubbles, nanocups, droplets and echogenic liposomes. When exposed to ultrasound pressure waves, gas-filled nuclei respond by expanding and contracting volumetrically, and droplets vaporize into microbubbles. Microbubble oscillations and acoustic droplet vaporization impart theragnostic potential because this characteristic response can both be detected by clinical diagnostic ultrasound scanners and locally enhance treatment by inducing cellular responses (Sutton et al. 2013; Kooiman et al. 2014, Wang et al. 2018a). "Sonobactericide" describes the enhancement of bactericidal action aided by ultrasound and the presence of cavitation nuclei, both endogenous and exogenous. This terminology is consistent with the nomenclature of other therapeutic applications of ultrasound-activated cavitation nuclei such as sonoporation—the formation of micropores within cell membranes (Kooiman et al. 2014), sonothrombolysis—the lysis of thrombi (Sutton et al. 2013), sonoreperfusion—the restoration of perfusion after microvascular obstruction (Black et al. 2016) and sonodynamic therapy—the treatment of neoplastic cells using a sonosensitizer (Rosenthal et al. 2004). Sonobactericide, like the other approaches, can be used either alone or in combination with other drugs, such as antimicrobials.

Address correspondence to: Kirby R. Lattwein, Thoraxcenter Biomedical Engineering, Room Ee2302, Erasmus MC, University Medical Center Rotterdam, PO Box 2040, 3000 CA Rotterdam, The Netherlands. E-mail: k.lattwein@erasmusmc.nl

Sonobactericide arrives at a time when traditional microbial therapy is limited by the increasing prevalence of multidrug-resistant bacteria. There are several resistance mechanisms and a large contributing factor is the development of biofilms, bacterial communities encased in a complex extracellular polymeric matrix consisting of variable amounts of numerous constituents, such as polysaccharides and proteins. This matrix provides both a scaffold for antibiotic binding and an anoxic and acidic environment that can deactivate antibiotics and decrease bacterial susceptibility *via* a reduced metabolism (Algburi et al. 2017). In addition to the presence of a protective extracellular matrix, the large heterogeneity and general 3-D structure of a biofilm hinder antibiotic delivery, penetration and effectiveness. Additionally, it is difficult to diagnose bacterial infections before they become extensively established (Grant and Hung 2013; Werdan et al. 2014). Sonobactericide, as illustrated in Figure 1, may increase the "footprint" of antibiotic bactericidal action, directly kill bacteria and reduce treatment time.

This review focuses specifically on the principles of sonobactericide using exogenous cavitation nuclei for potential clinical translation. As this new line of research gains ground, it is pertinent to establish important considerations for future work. Main concepts of the variability of bacteria, microbubble composition and acoustic behavior and ultrasound parameters are addressed, and the experimental setups and measured outcomes are evaluated. Articles on sonobactericide published before August 2019 were identified using PubMed, Web of Science and Google Scholar search engines with the keywords "ultrasound," "microbubble" (or "bubble" or "contrast") and "bacteria" or "biofilm." Sonobactericide articles referenced by those found in our search were also included. Articles were excluded if they were not written in English or if ultrasound alone, that is, without added cavitation

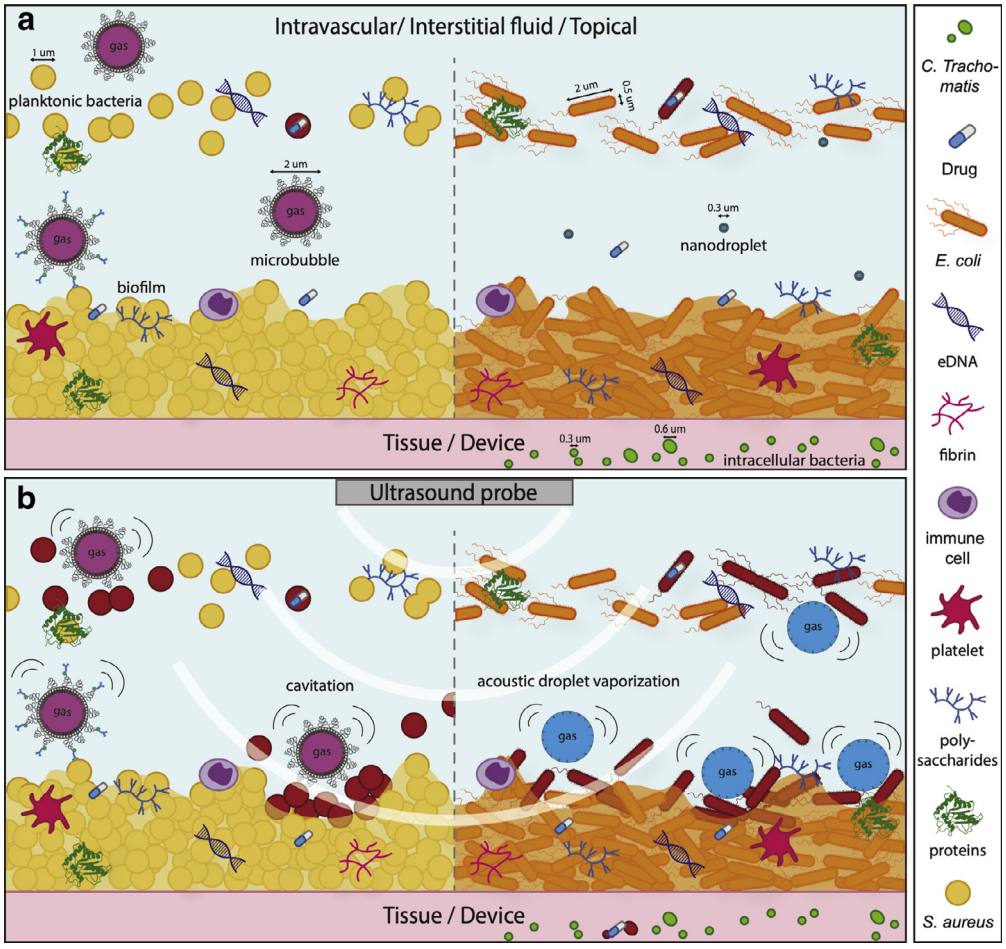

Fig. 1. Concept of sonobactericide (not drawn to scale). (a) Potential infection environments before ultrasound. Sizing of bacteria and cavitation nuclei is denoted with a *double-headed arrow*. (b) Ultrasound application in which cavitating microbubbles and activated nanodroplets disrupt bacteria and biofilm composition. Bacteria that have become red in (b) are considered dead or to have compromised membranes because of the effects from ultrasound and cavitating nuclei.

nuclei (*i.e.,* microbubbles or droplets), was investigated as a potential application for treatment. For treatment with ultrasound alone, the reader is referred to other excellent reviews (Erriu et al. 2014; Cai et al. 2017; Vyas et al. 2019). Twenty-seven sonobactericide articles were selected for this review (Table 1). One article that investigated microbubbles targeted to biofilm for diagnostic application (Anastasiadis et al. 2014) and six articles that studied the effect of cavitation nuclei on bacteria without ultrasound (Cavalieri et al. 2008, 2012, 2013; Zhou et al. 2012; Mahalingam et al. 2015; Argenziano et al. 2017) were excluded from Table 1 because these studies did not meet our definition of sonobactericide.

BACTERIA

There exists a vast diversity among bacteria; even closely related bacteria can have different morphologies, metabolisms and defenses. Considering shape morphology, besides the familiar rod (bacillus), spherical (coccus) and spiral (twisted) types, at least six other general shapes exist (Kysela et al. 2016). Though current sonobactericide research into pathogenic bacteria is dominated by bacillus- and coccus-shaped bacteria, infectious diseases are also caused by bacteria with other morphologies. Microbubbles may oscillate differently when paired with similarly spherical-shaped *Staphylococcus aureus*, versus rod-shaped *Escherichia coli* or the junction of the kidney-shaped diplococcus *Neisseria meningitidi*s because of total surface area contact, tension and rigidity. These shape differences along with variation in cell surface could influence treatment success. For example, fimbriae are bristle-like external filamentous structures protruding from some bacterial cell surfaces which may create a stand-off distance between the cavitation nuclei and cell wall. It has been observed that as the initial stand-off distance increases, biofilm disruption, sonoporation and cytoskeleton disassembly decrease (Goh et al. 2015; Wang et al. 2018b). Moreover, microbubble dynamics also depend on the distance from and material properties of a surface (Overvelde et al. 2011; van Rooij et al. 2017).

Based on the cell envelope (a multilayered structure on the outside of the cell), almost all bacteria can be subdivided into two main groups: Gram+ or Gram−. The cell envelope of Gram+ bacteria consists of a thick (20−80 nm) peptidoglycan layer, which is threaded with teichoic acid, but lacks an outer membrane, as illustrated in Figure 2a. Peptidoglycan is made up of repeating units of muramic acid, which are cross-linked by peptide side chains. Gram− bacteria are covered by a thin peptidoglycan cell wall (<10 nm), surrounded by an outer lipid bilayer membrane containing pores, lipoproteins and lipopolysaccharide (Silhavy et al. 2010), as illustrated in Figure 2b. It is possible that these structural differences between Gram+ and Gram− bacteria will also result in dissimilar responses to sonobactericide. Several studies have compared treatment efficacy on both bacteria types (Mai-Prochnow et al. 2016), including ultrasound (67 and 20 kHz) paired with antibiotics without exogenous cavitation nuclei (Pitt et al. 1994; Liao et al. 2018), and observed a markedly different response. Furthermore, the size of the bacteria (~0.5−5 μm), whether a single bacterium, dividing bacterium or aggregates of several bacteria, and its location (in a suspension, on a surface, or intracellular) could have an impact on the therapeutic effectiveness of sonobactericide.

Seemingly subtle differences within a group of eukaryote cells can affect the differential reaction to oscillating microbubbles. This variable cell response to microbubbles is supported by sonoporation studies that have reported differences in drug delivery efficiency in two different cancer cell lines (Escoffre et al. 2011). The top three types of bacteria on which sonobactericide has been evaluated are (i) *Staphylococcus epidermidis* (Gram+, 7 studies, 26%); (ii) *S. aureus* (Gram+, 6 studies, 22%); and (iii) *E. coli* (Gram−, 4 studies, 15%) (Table 1). Methicillin-resistant *S. epidermidis* was employed in the majority of the studies (6 out of 7), whereas methicillin-resistant *S. aureus* (MRSA) was used in 4 of the 6 studies. Two research teams used a green fluorescent protein containing Gram− strain (*E. coli, Pseudomonas aeruginosa*) (Tandiono et al. 2012; Ronan et al. 2016). The majority of the studies used only one type of bacteria. Only one study used mixed types of bacteria (Agarwal et al. 2014). Two articles compared two different types of bacteria (Zhu et al. 2013; Li et al. 2015), and another compared a bacterium and a fungus (Tandiono et al. 2012). Only four studies used patient-derived clinical isolates originating from a central venous catheter (Hu et al. 2018b), infective endocarditis blood culture (Lattwein et al. 2018), pneumonia-induced sputum (Fu et al. 2019) and urine from a patient with lower urinary tract symptoms (Horsley et al. 2019). With the exception of Agarwal et al. (2014), who used bacteria from a wastewater reclamation plant to investigate membrane biofouling removal, the other groups used lab-derived strains, which may limit clinical applicability. Though a laboratory strain may be deemed wild type, the preparation and (worldwide) dissemination can lead to genetic changes that cause both disruption of virulence regulatory pathways, which often imparts loss of typical *in vivo* virulence potential, and phenotypic variation among an entire strain pedigree (Bæk et al. 2013). Also, typing clinical isolates, such as staphylococcal protein A (*spa*) typing performed by Lattwein et al. (2018) or core-genome multilocus sequence typing, would aid in the verification of disease association.

Table 1. Overview of sonobactericide papers

Pathogen type	Pathogen	Culture type	*In vitro*	*In vivo*	Model setup	Antimicrobial	Cavitation nuclei	US frequency (MHz)	Pressure/intensity or calculated pressure	Cycles/PRF/ treatment time	Ref.
Gram+	*Enterococcus faecalis*	Biofilm	X	-	Root canals of single-rooted polymer and human teeth	5.25% NaOCl	Custom-made	0.032 ± 0.004	N.D.	N.D., 1 min	Halford et al. 2012
		Intracellular	X	-	Infected human bladder cell organoid model	Gentamicin	Custom-made	1.1	2.5 MPa	25% duty cycle, PRF 50 Hz, 20 s	Horsley et al. 2019
	Propioni bacterium acnes	Planktonic; *in vivo*: N.D.	X	X	Eppendorf tube; intradermally into mouse ears	Lysozyme	Custom-made	1	*In vitro*: 1, 2, 3 W/cm^2 *In vivo*: 3 W/cm^2	50% duty cycle, *in vitro*: 1 min; *in vivo*: 1 min, q.d. for 13 d	Liao et al. 2017
	Staphylococcus aureus	Planktonic	X	X	Tissue culture plate; bone cement in rabbit tibiae	Vancomycin	SonoVue	1	0.3 W/cm^2	30% duty cycle, 24 h	Lin et al. 2015
		Biofilm	X	-	Tissue culture plate/ coverslip	Vancomycin	Custom-made	1	0.3 W/cm^2	50% duty cycle, 5 min	Guo et al. 2017
		Biofilm	X	-	Infected clot on a suture in glass capillaries	Oxacillin	Definity	0.12	0.44 MPa (PTP)	Continuous wave, 50 s on 30 s off, 30 min	Lattwein et al. 2018
		Biofilm	-	X	Subcutaneously implanted titanium plate in mice	Human β- defensin 3	Custom-made/ SonoVue	0.08	0.2 W/cm^2	50% duty cycle, 20 min, t.i.d. for 7, 14, 28 d	Zhou et al. 2018
	Staphylococcus epidermidis	Biofilm	X	X	Tissue culture plate; subcutaneously implanted disk in rabbits	Vancomycin	SonoVue	0.08	*In vitro*: 1 W/cm^2 *In vivo*: 0.5 W/cm^2	50% duty cycle, *in vitro*: 10 min; *in vivo*: 20 min, t.i.d. for 72 h	He et al. 2011
		Biofilm	X	-	OptiCell	Vancomycin	Custom-made	0.3	0.5 W/cm^2 or 0.12 MPa*	50% duty cycle, 5 min	Dong et al. 2013
		Biofilm	X	-	OptiCell	Vancomycin	Custom-made	1	0.5 W/cm^2 or 0.12 MPa*	50% duty cycle, 5 min	Dong et al. 2017
		Biofilm	-	X	Subcutaneously implanted catheter in rabbits	Vancomycin	Custom-made	0.3	0.5 W/cm^2 or 0.12 MPa*	50% duty cycle, 5 min, b.i.d. for 48 h	Dong et al. 2018
		Biofilm	X	-	Tissue culture plate; glass FluoroDish	Vancomycin	SonoVue	1	1 W/cm^2 or 0.24 MPa*	50% duty cycle, 10 min	Hu et al. 2018b
	S. aureus and *S. epidermidis*	Biofilm	X	-	Tissue culture plate with titanium plate	Human β-defensin 3	SonoVue	0.08	1 W/cm^2	50% duty cycle, 10 min	Zhu et al. 2013
		Biofilm	-	X	Subcutaneously implanted titanium plate in mice	Human β-defensin 3	SonoVue	0.08	0.2 W/cm^2	50% duty cycle, 20 min, t.i.d. for 48 h	Li et al. 2015
	Streptococcus mutans	Biofilm	X	-	Tissue culture plate with disk	None	Sonazoid	0.28	N.D.	0-90% duty cycle, 1 min	Nishikawa et al. 2010
Gram−	*Acinetobacter baumannii*	Biofilm	X	-	Tissue culture plate/ coverslip	Polymyxin B	Custom-made	1	3 W/cm^2	continuous wave, 5 min	Fu et al. 2019
	Chlamydia trachomatis	Intracellular	X	-	Infected HeLa cells in tissue plate with gas-permeable bottom	Doxycycline; ceftizoxime	Custom-made	1.011	0.15, 0.44 W/cm^2 or 0.13, 0.23 MPa†	25% duty cycle, 20 sec	Ikeda-Dantsuji et al. 2011
	Escherichia coli	Planktonic	X	-	Centrifuge tubes	None	Albunex; ST68 custom-made	1	500 W/cm^2	1ms pulse, PRF 20 Hz, 5 min	Vollmer et al. 1998
		Planktonic	X	-	Tubes	Gentamicin	SonoVue	0.0465	0.01 W/cm^2	33% duty cycle, 12 h	Zhu et al. 2014

(*continued on next page*)

Table 1 (***Continued***)

Pathogen type	Pathogen	Culture type	*In vitro*	*In vivo*	Model setup	Antimicrobial	Cavitation nuclei	US frequency (MHz)	Pressure/intensity or calculated pressure	Cycles/PRF/ treatment time	Ref.
		N.D.	-	X	Direct injection into rat prostates	None	Custom-made	1	0.5 MPa / 0.023 W/cm^2	1% duty cycle, 5 min	Yi et al. 2016
		N.D.	-	X	Intratracheally infected mice	Gentamicin	Definity	1.3	0.9−1.2 MPa (PNP)	Pulse every 5 s, 5 min	Sugiyama et al. 2018
	Fusobacterium nucleatum	Planktonic	X	-	Tissue culture plate	None	Optison	0.96	0.5 MPa (PPP)	50% duty cycle, PRF 1 Hz, 90 s	Han et al. 2005
		Planktonic	X	-	Tissue culture plate	None	Definity	1	0.25, 0.5, >0.9 MPa (PPP)	0−50% duty cycle, PRF 1−100 Hz, 10, 90, 450 s	Han et al. 2007
	Pseudomonas aeruginosa	Biofilm	X	-	Glass coverslip in flow cell	Gentamicin; streptomycin	Definity	0.5	1.1 MPa (PNP)	16 cycle tone burst, PRF 1 kHz, 5 min	Ronan et al. 2016
	Pseudomonas putida	Biofilm	X	-	Glass coverslip in acetate film chamber	None	SonoVue	0.25, 1	0.1, 0.5, 0.7 MPa (PNP)	50 μs pulse	Goh et al. 2015
	E. coli and *Pichia pastoris* (yeast)	Planktonic	X	-	Microfluidic system	None	Custom-made	0.13	10 bar (~1 MPa)	500−50,000 cycles, ms−s, every 5 s	Tandiono et al. 2012
Mixed	N.D.	Biofilm	X	-	Nylon membrane surface	None	Custom-made	0.042	N.D.	2s pulse, every 2 min, 15 min	Agarwal et al. 2014

US = ultrasound; PRF = pulse repetition frequency; N.D. = not defined; PTP = peak-to-peak pressure; PPP = peak-positive pressure; PNP = peak-negative pressure; q.d. = once daily; b.i.d. = twice daily; t.i.d. = thrice daily; I_{SPTA} = spatial pulse-average intensity; I_{SATA} = spatial-average temporal-average intensity.

* Calculated peak pressure from I_{SPTA} values obtained by personal communication with author(s). Calculations were performed using the formula (Kinsler et al. 2000) $I_{SPTA} = I_{SATA}$/duty factor.

† Calculated peak pressure from I_{SATA} values obtained by personal communication with author(s). Calculations were performed using the formula (Kinsler et al. 2000) $I_{SATA} = P^2/2\rho c$, where p denotes the peak pressure, and ρ and c denote the density and speed of sound.

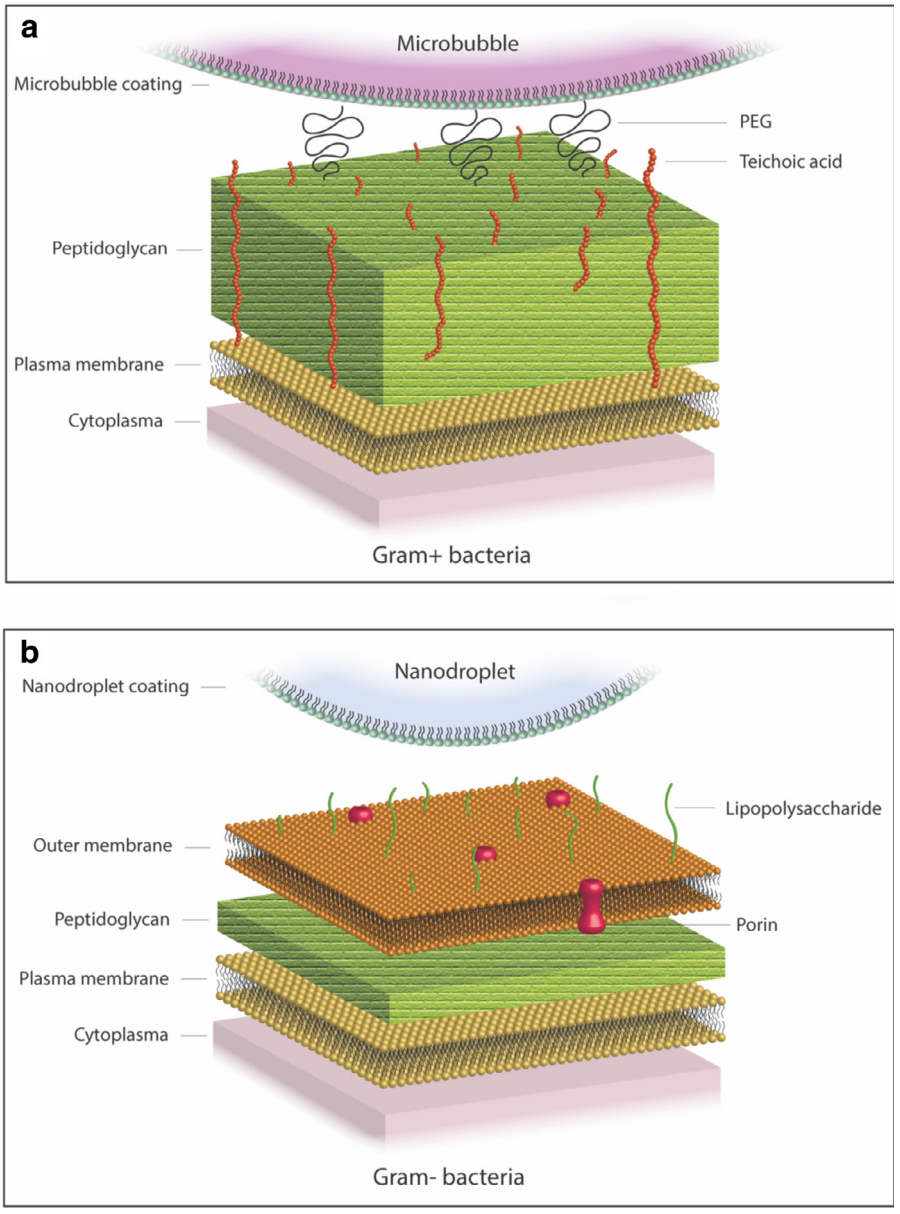

Fig. 2. Interaction of cavitation nuclei with bacteria: (a) interaction between phospholipid-coated microbubbles and Gram+ bacteria, (b) interaction between phospholipid-coated nanodroplets and Gram− bacteria. PEG = polyethylene glycol.

Three modes of growth exist for bacteria: planktonic, associated with a surface and intracellular. Bacteria in different growth modes have distinctly different characteristics. Planktonic refers to free living bacterial cells, which can occur in two forms: as single bacterial cells or in clusters known as planktonic aggregates (Crosby et al. 2016). Clinically, this planktonic mode generally refers to bacteria that gain entrance to the human body in the bloodstream and cause bacteremia, which results in acute infections often effectively treated by the host immune system and antibiotics (Stewart and Costerton 2001; Brady et al. 2018). Seven sonobactericide studies (26%) focused on planktonic bacteria (Table 1).

In contrast, bacteria adhering to living (biotic) and non-living (abiotic) surfaces cover themselves with a protective matrix, classically known as a biofilm. Bacteria in a biofilm are protected against attacks from the immune system and are up to 1000 times more resistant to antimicrobial therapy than planktonic bacteria (Lewis 2005). Biofilm formation is abundant, and an estimated 60% of human bacterial infections are biofilm related (Costerton et al. 1999; Fux et al. 2003). Correspondingly, 63%

(17/27) of the sonobactericide studies focused on treatments for biofilm infections. Biofilm can occur on teeth; native and prosthetic heart valves; medical implants, such as prosthetic joints, surgical mesh and screws; pacemakers; and indwelling catheters (Lebeaux et al. 2014). These biofilms consist of surface aggregates of bacteria imbedded in an extracellular matrix of sugars of bacterial origin, extracellular DNA and proteins, both originating from either the host or the bacteria. For instance, when *S. aureus* is exposed to blood, the coagulation cascade is activated by coagulase produced by the bacterium. The fibrin forms a scaffold to which the bacteria bind, facilitating the formation of a biofilm (Zapotoczna et al. 2016). Other biofilm composition examples include *Pseudomonas aeruginosa* forming sputum-encased biofilms surrounded by immune cells in lungs affected by cystic fibrosis (Maurice et al. 2018), and *Proteus mirabilis* forming crystalline biofilms by inducing urinary salt precipitation in the catharized urinary tract (Delcaru et al. 2016). Biofilm extracellular matrix composition and architecture are complex and highly influenced by species/strain/lineage, developmental conditions, nutrient availability, cell−cell signaling and interactions with the (host) environment (Magana et al. 2018). Moreover, most biofilm infections are polymicrobial (Short et al. 2014), which adds to the microenvironment complexity. The various processes driving bacterial responses are not completely understood. Thus simulating human *in vivo* biofilms remains highly challenging (Bjarnsholt et al. 2013; Roberts et al. 2015).

There are indications that bacteria in a single biofilm do not behave *en groupe*. Archer et al. (2011) found that *S. aureus* biofilms contain cells in at least four distinct metabolic states: aerobic, fermentative, dormant (including very slow growing cells and persisters) or dead. It is likely that bacterial cells in different metabolic states, stages of cell division or growth phases will respond differently to sonobactericide. This hypothesis is supported by the observation that planktonic bacteria in stationary growth phase are more resistant to ultrasound alone or combined with cavitation nuclei (Vollmer et al. 1998).

Bacteria can be dispersed from mature biofilms and become planktonic again (Otto 2008). Dispersal agents, including chemical, enzymatic and mechanical methods, can also be used to make biofilm bacteria more susceptible to therapeutics. Recent literature on *P. aeruginosa* suggests that bacteria dispersed from biofilms have a physiology different from those of both planktonic and biofilm growth modes (Chua et al. 2014). This difference suggests a possible transitional growth mode for bacteria acclimating to the planktonic state. These researchers found that the dispersed cell phenotype was highly virulent and remained for at least 2 h. This finding is supported further by studies that manipulated biofilm dispersal, which led to increased disease severity and progression in mice and a transition from asymptomatic colonization to active infection, respectively (Connolly et al. 2011; Marks et al. 2013). Chua et al. (2014) discovered that dispersed cells exhibited lower iron uptake gene expression and paired the dispersal agent with an iron chelator, which led to significant reduced viability. Other work revealed that dispersed bacteria exhibited increased antibiotic susceptibility and, only after lag phase ($\geq$3 h), were more active (Lee et al. 2018). Thus, biofilm dispersal should be considered and investigated for sonobactericide development.

EXPERIMENTAL APPROACHES

The first to report sonobactericide in combination with an antimicrobial was Ikeda-Dantsuji et al. in 2011. Since then, 18 articles on sonobactericide using antimicrobials have been published (Table 1). The most studied clinical antibiotic was vancomycin (7 studies, 26%). Six other antibiotics were investigated, with different ones for Gram+ and Gram− bacteria except gentamicin. Two groups investigated two antibiotics separately on the same bacterial strain. Ikeda-Dantsuji et al. (2011) investigated one antibiotic to which the *Chlamydia trachomatis* strain was susceptible (doxycycline) and one to which this bacterial strain was resistant (ceftizoxime). Ronan et al. (2016) used two aminoglycosides (gentamicin and streptomycin) to which the *P. aeruginosa* PAO1 strain was susceptible as determined by CO_2 metabolic production.

In addition to the antibiotics, three other antimicrobials were investigated: sodium hypochlorite (NaOCl), lysozyme and human β-defensin 3 (Table 1). The studies included either clinically appropriate antimicrobials (dental, NaOCl [Halford et al. 2012]) or antimicrobials testing a new approach (lysozyme [Liao et al. 2017]; human β-defensin 3, [Zhu et al. 2013, Li et al. 2015, Zhou et al. 2018]). Sodium hypochlorite is a disinfectant used widely in endodontic irrigation and health care facilities (Estrela et al. 2002). Human β-defensin 3, an endogenous broad-spectrum antimicrobial peptide produced by various cells in the human body (Dhople et al. 2006), was administered in free form or encapsulated in liposomes (Zhou et al. 2018). The aim was to load the liposomes onto SonoVue microbubbles, but proof thereof was not provided. Lysozyme is a naturally occurring antimicrobial protein and was used in five (non-sonobactericide) papers as the microbubble coating material (Cavalieri et al. 2008, 2012, 2013; Zhou et al. 2012; Mahalingam et al. 2015).

All sonobactericide studies used an appropriate antibiotic targeting a specific microbe, according to therapeutic guidelines (Mandell et al. 2000; Mermel et al.

2009; Osmon et al. 2012; Baddour et al. 2015; Habib et al. 2015; Lanjouw et al. 2016), excluding 2 studies that could not be linked to guidelines because of nondisclosure of microbe information beyond species (Lin et al. 2015) and no disease aim (Zhu et al. 2013). Two examples of correct antibiotic and microbe pairings are found in Sugiyama et al. (2018), who aimed to treat severe Gram− bacterial pneumonia and used an *E. coli* strain for which the Canadian guideline recommends gentamicin (Mandell et al. 2000), and Lattwein et al. (2018), who aimed to treat infective endocarditis and used a methicillin-susceptible *S. aureus* isolate for which both the European (Habib et al. 2015) and American (Baddour et al. 2015) guidelines recommend oxacillin. Additionally, of the studies using an antibiotic, 2 of 9 focusing on Gram+ bacteria used strains already resistant to first-line antibiotics. Many infections are not dominated by resistant microbes, and Gram− bacteria can have higher resistance profiles than Gram+ bacteria (Hu et al., 2018a). This choice could be influenced by media coverage, strain access or geographic location. All articles using vancomycin and methicillin-resistant microbes originated from China, which has high levels of reported antimicrobial resistance (Hu et al., 2018a).

A few groups performed sonobactericide using non-antimicrobial therapeutics. One paper used recombinant tissue plasminogen activator (rtPA), a clinically approved fibrinolytic agent, in combination with the antibiotic oxacillin (Lattwein et al. 2018). Two articles investigated gene transfection of plasmid DNA into planktonic bacteria (Han et al. 2005, 2007). The microbubble-mediated accumulation of bone marrow mesenchymal stem cells, which can suppress inflammation, was investigated as a treatment for chronic bacterial prostatitis (Yi et al. 2016). Although the majority of sonobactericide studies paired their treatments with therapeutics, 5 (19%) focused directly on the mechanical and biological effects resulting from ultrasound and microbubbles alone (Vollmer et al. 1998; Nishikawa et al. 2010; Tandiono et al. 2012; Agarwal et al. 2014; Goh et al. 2015).

Many of the *in vitro* studies were performed in polystyrene tissue culture well-plates, ranging from 96- to 6-well plates, for both planktonic and biofilm studies (10 studies, 37%; Table 1). To the well-plates, Zhu et al. (2013) added a 10-mm diameter titanium plate (1 mm thick); Guo et al. (2017) a 13-mm glass coverslip; Fu et al. (2019) a 12-mm glass coverslip; and Nishikawa et al. (2010) a polystyrene disk (dimensions not provided). Two studies also cultured biofilm in a FluoroDish, a 35-mm dish containing a 23.5-mm glass window (He et al. 2011; Hu et al., 2018b). The geometry of both these containers could result in the reflection of ultrasound at the bottom of the well and at the medium−air interface. As a result, constructive and deconstructive interference leading to standing waves could have occurred (Coakley et al. 1989). Standing waves may also form within the body, especially in the presence of bone (O'Reilly et al. 2010). Microbubbles may aggregate at the nodes of a standing wave (Shi et al. 2013). Increases in *in situ* acoustic pressure caused by constructive interference can cause unwanted bio-effects mediated by inertial cavitation (Azuma et al. 2005; Deffieux and Konofagou 2010). The presence of standing waves produces acoustic field variations that are sensitive to changes in transducer position, excitation frequency or temperature (Huber et al. 2011). The acoustic intensity of the ultrasound field is proportional to the square of the pressure amplitude when the ultrasound wavelength is much smaller than the transducer aperture (Kleven et al. 2019). Under the plane wave approximation, the acoustic pressure is related to the intensity as follows: $I = P^2/2pc$, where P is the peak acoustic pressure, p is the density and c is the speed of sound (Kinsler et al. 2000). For traveling waves, the intensity is a function of time; that is, once the wave has passed a given spatial location, the intensity drops to zero. However, for standing waves, the peak intensity at a spatial location remains constant over time. Effects of standing wave formation during insonation of cells in different holders have previously been investigated in detail (Hensel et al. 2011).

Measurement of *in situ* acoustic parameters is critical to understanding treatment effects, correlating the treatment effects to specific outcomes and translating these to an *in vivo* setting (ter Haar et al. 2011). Only 5 sonobactericide studies reported calibrating the output *in situ* (Tandiono et al. 2012; Goh et al. 2015; Ronan et al. 2016; Lattwein et al. 2018; Horsley et al. 2019). The lack of standardization of exposure setups makes it difficult to compare the results in the literature. Reporting spatial maps of the acoustic field *in situ* could help improve the reproducibility and interpretation of *in vitro* studies between groups (ter Haar et al. 2011).

In the well-plates and FluorDishes, cavitation nuclei were administered once for treatment times varying from 20 s to 10 min (see Table 1), with the exception of one study in which fresh microbubbles were administered every 4 h for 24 h (Lin et al. 2015). It is unclear whether microbubbles were still present beyond a few minutes during insonification because of destruction or dissolution. For example, Mannaris and Averkiou (2012) reported that SonoVue microbubbles, insonified *in vitro* for 20 ms at 1 MHz using 10 cycle pulses at a pulse repetition frequency (PRF) of 100 Hz, were destroyed and/or dissolved after only a few pulses at 400 kPa acoustic pressure, whereas microbubbles were still present after all pulses at an acoustic pressure of 100 kPa. In addition, pulses longer than 100 cycles at acoustic pressures >0.4

did not give any added benefit in terms of microbubble oscillation. One group used the OptiCell cell culture system for their biofilm experiments (Dong et al. 2013, 2017), which consists of two gas-permeable, thin (75 μm) polystyrene membranes, spaced parallel and 2 mm apart, providing 50 cm^2 area of cell culture. Microbubbles were administered once for a 5 min treatment (0.3 or 1 MHz, 0.12 MPa, 50% duty cycle) period.

Several groups used a less commercial *in vitro* setup. Goh et al. (2015) used an acetate film square chamber with the top and right sides each consisting each of a coverslip and the ultrasound (250 kHz or 1 MHz, 0.1−1 MPa, 50-μs pulse) transducer positioned below. One coverslip had a biofilm, such that the microbubbles were either floating beneath the biofilm or optically trapped at varying distances from the side. Lattwein et al. (2018) performed sonobactericide under plasma flow (0.65 mL/min) on biofilms grown statically on human whole blood clots placed in glass capillaries (2.15-mm inner diameter). Microbubbles were continuously infused, and ultrasound (120 kHz, 0.44 MPa, continuous wave, 50 s on 30 s off) was applied intermittently for 30 min. Ronan et al. (2016) grew biofilms in a cylindrical flow cell (17 mL/h) with an acoustically transparent membrane on one side and a glass coverslip on the other, and flow was halted to perform sonobactericide (0.5 MHz, 1.1 MPa, 16-cycle tone burst, PRF = 1 kHz) for 5 min, with microbubbles administered once. Flow was also used by Tandiono et al. (2012) to treat planktonic bacteria in a microfluidic system composed of polydimethylsiloxane-made channels. In humans, biofilms can develop in variable fluid flow environments depending on the location or under static conditions. Biofilms are highly sensitive to these different conditions (Thomen et al. 2017). Thus, selection of the appropriate static or flow condition setting should be tailored to the specific aimed application, such as superficial skin wound or intravascular device infections.

For dental application, Halford et al. (2012) grew biofilms in the root canal (12 mm length) of single-rooted extracted human teeth under constant agitation (120 rpm). Microbubbles were delivered into canals and insonified with a P5 Newtron dental ultrasonic hand piece (28 to 36 kHz ultrasound) for 1 min. Horsley et al. (2019) employed a bladder organoid model using a modified acoustically compatible chamber (Carugo et al. 2015). Briefly, a polycarbonate filter insert (12 mm diameter) cultured with infected human bladder cells was fixed between an Ibidi culture dish (35 mm) and a polydimethylsiloxane lid. Cavitation nuclei were added, and the dish and lid were coupled and then insonified (1.1 MHz, 2.5 MPa, 5500 cycles, 20 ms pulse duration) for 20 s. Other *in vitro* experimental setups were on nylon membranes (47 mm diameter, pore size = 0.2 μm) and in centrifuge tubes (2 and 5 mL) (Table 1). Nylon membrane biofilms were treated in a beaker placed in a sonicator (0.042 MHz, on for 2 s every 2 min) while microbubbles were continuously introduced for 15 min (Agarwal et al. 2014). The planktonic bacteria in tubes were treated (1 MHz, 500 W/cm^2, 2% duty cycle) for 5 min (Vollmer et al. 1998) or 12 h (0.0465 MHz, 0.01 W/cm^2, 33% duty cycle) (Zhu et al. 2014) and in Eppendorf tubes (1 MHz, 1−3 W/cm^2, 50% duty cycle) for 1 min (Liao et al. 2017), all with a one-time administration of microbubbles.

Three *in vitro* studies were followed up with a corresponding *in vivo* study in the same article (He et al. 2011; Lin et al. 2015; Liao et al. 2017). Thirty percent of the articles on sonobactericide (8/27) have investigated therapeutic efficacy in pre-clinical animal models (Table 1). Four groups chose to emulate implanted medical device infections using subcutaneous implants, near the spine, with biofilm grown on catheter pieces or polyethylene disks in rabbits (He et al. 2011, Dong et al. 2018) and titanium plates in mice (Li et al. 2015; Zhou et al. 2018). Microbubbles were injected subcutaneously into the implant area before ultrasound. For each of the three ultrasound exposures (20 min) per day, He et al. (2011) injected 200 μL of microbubbles (2×10^8 to 5×10^8/mL) every 5 min, and both Li et al. (2015) and Zhou et al. (2018) injected 30 μL once, 2×10^8 to 5×10^8/mL and concentration not disclosed, respectively. Dong et al. (2018) applied ultrasound twice a day for 5 min, and injected 500 μl (1.2×10^9/mL diluted to 1% v/v) each time. All studies used a 50% duty cycle. However, acoustic parameters, treatment intervals and duration times varied (Table 1).

Lin et al. (2015) investigated the ability of sonobactericide to increase the elution rate of antibiotics from vancomycin-loaded bone cement in a periprosthetic infection rabbit tibia model. Ultrasound (1 MHz, 0.3 W/cm^2, 30% duty cycle) was applied transcutaneously for 24 h, and microbubbles (2×10^8 to 5×10^8/mL) were injected into the same space as the *S. aureus* bacteria at four time points. Surrounding tissues were evaluated directly after treatment. For chronic bacterial prostatitis modeled in rats, Yi et al. (2016) used sonobactericide to induce accumulation of bone marrow mesenchymal stem cells to reduce inflammatory reactions and resolve infection. After 4 wk of infection induction with *E. coli*, microbubbles (0.1 mL/kg) were directly injected into prostates and insonified (1 MHz, 0.5 MPa, 1% duty cycle) for 5 min. Afterward, stems cells (1×10^7) were administered intravenously, and therapeutic effectiveness was evaluated after 24 h and 2 wk.

Another study focused on harnessing sonobactericide in a model of severe bacterial pneumonia with the goal of enhancing antibiotic delivery to infected lung

tissue in mice (Sugiyama et al. 2018). *E. coli* were administered intratracheally, and 6 h later gentamicin was injected intraperitoneally. After 30 min, microbubbles (1×10^9) were intravenously administered and ultrasound (1.3 MHz, 0.9−1.2 MPa, pulse every 5 s; pulse duration not specified) was transmitted thoracically for 5 min. Lavage and tissues samples were evaluated at 30 min and 2 h, respectively, after ultrasound application. Liao et al. (2017) also used mice and aimed to improve acne vulgaris treatment using transdermal sonobactericide with lysozyme-shelled microbubbles. Ears were infected intradermally with *Propionibacterium acnes*. Gel loaded with lysozyme microbubbles was placed on top of the infected area and insonified (1 MHz, 3 W/cm^2, 50% duty cycle) daily for 1 min. Effectiveness was assessed at several time points during the 13 d of treatment.

Various techniques were used for assessing sonobactericide efficacy. The colony-forming unit plate-counting method was utilized to determine antimicrobial efficacy (14/27, 52%), for some *in vitro* and all except one *in vivo* study (Yi et al. 2016). Bacterial plating is relatively easy to perform and considered the "gold standard" for determining viable bacteria counts. This technique, however, is widely known to underestimate the absolute number of bacteria. Another potential limitation is that often to obtain post-treatment samples, biofilms have been mechanically disrupted, scraped, centrifuged, digested, vortexed or sonicated, which might have induced microbial alterations. Several articles employed histopathologic staining, either crystal violet or hematoxylin and eosin, to observe bacterial morphology (macroscopy and light microscopy), quantify biofilm density by absorbance levels in a microplate reader or compare inflammatory effects over time. This method can be used for high-throughput screening, but it does not discriminate between live and dead cells. Immunohistochemistry was used by Yi et al. (2016) to quantify inflammatory cytokine expression and distribution. Agarwal et al. (2014) desiccated their mixed species biofilms to determine fixed biomass for overall density quantification and also, albeit with additional steps, for extracellular protein and polysaccharide content.

Several microscopic techniques were utilized for visualization of treatment, including light, epifluorescence, confocal laser scanning and transmission and scanning electron microscopy. Light microscopy was combined with or without time-lapse and high-speed camera observations (Halford et al. 2012; Tandiono et al. 2012; Goh et al. 2015; Lattwein et al. 2018); see Figure 3 for a light microscopy example. Fluorescence detection, with either a widefield or a confocal microscope, was the most frequently utilized optical imaging modality for qualitative and quantitative visualization of live and fixed cell populations (16/27, 59%). These images can provide information not only on viability, but also biomass, average biofilm thickness and structural heterogeneity. Live/dead nucleic acid staining with Syto 9 (viable cells) and propidium iodide (dead or membrane-disrupted cells) were often used and the cells were observed with confocal microscopy (Fig. 4) to assess biofilm populations. Note that biofilm nucleic acid fluorescence signals might not only indicate a single bacterium, but also extracellular DNA found throughout many biofilms (Okshevsky and Meyer 2014). To investigate biofilm compositional changes, extracellular proteins were stained with fluorescein isothiocyanate (FITC), lipids with Nile red and α- and β-polysaccharides with lectin concanavalin A conjugated with tetramethyl rhodamine and fluorescence brightener, respectively (Agarwal et al. 2014). These polysaccharides (α, β) can also be visualized with FITC-conjugated lectin concanavalin A and wheat germ agglutinin (Anastasiadis et al. 2014). Scanning and transmission electron microscopy was used for post-treatment ultrastructural observations of planktonic bacteria and biofilm

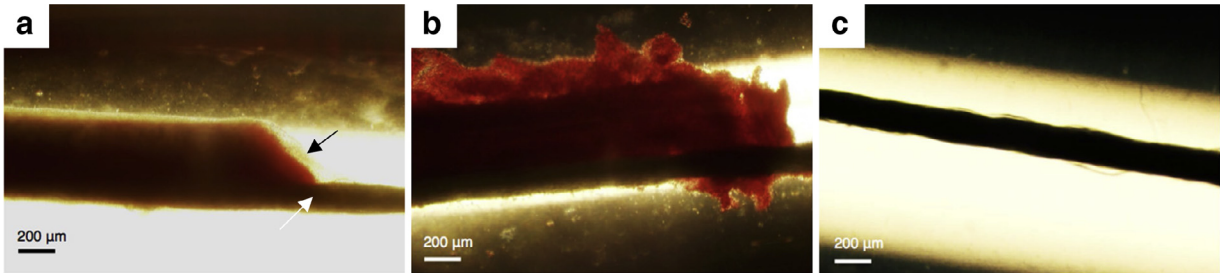

Fig. 3. Bright-field micrographs of *in vitro*-produced *Staphylococcus aureus*-infected clots after a 30-min treatment with (a) plasma alone; (b) plasma, recombinant tissue plasminogen activator (rt-PA, thrombolytic) and oxacillin (antibiotic); and (c) plasma, rt-PA, oxacillin, ultrasound and Definity (microbubble). The *black arrow* in (a) indicates the biofilm (beige). The *thick black line*, seen in all images and denoted by a *white arrow* in (a), is the suture to which the respective infected clots were adhered. Ultrasound parameters were 0.12 MHz and 0.44 MPa peak-to-peak pressure, intermittent (50 s on, 30 s off) continuous waves for 30 min. Adapted, with permission, from (Lattwein et al. 2018).

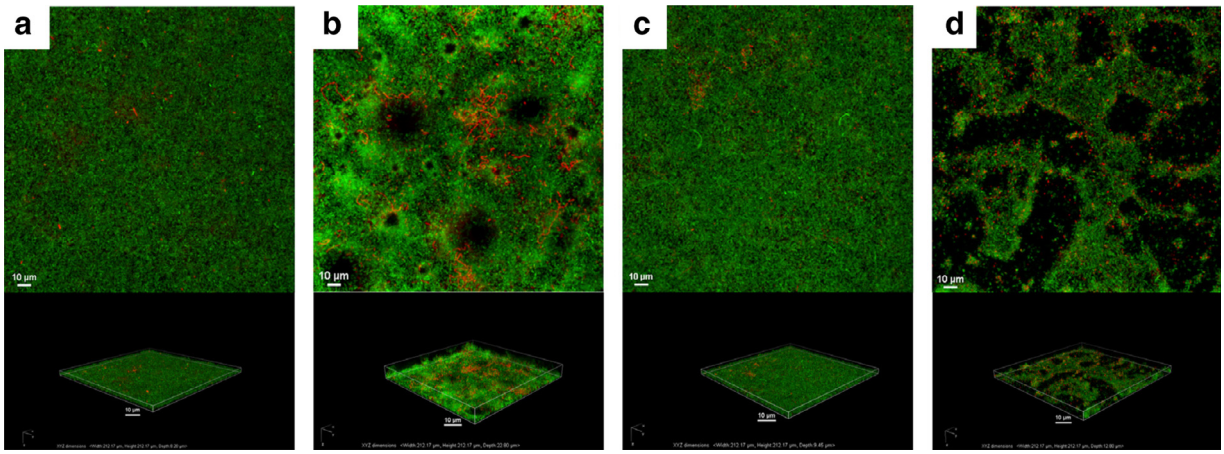

Fig. 4. Confocal laser scanning micrographs of *in vitro*, propidium iodide (red)-stained *Pseudomonas aeruginosa* PAO1: gfp-2 biofilms after treatment with (a) nothing (control); (b) ultrasound and Definity (microbubbles); (c) gentamicin (antibiotic) alone; and (d) gentamicin, ultrasound and Definity. Top: Top-down maximum intensity projection. Bottom: Corresponding 3-SD volume rendering. Ultrasound parameters were 0.5 MHz at 1.1 MPa peak negative pressure with a 16-cycle tone burst and pulse repetition frequency of 1 kHz for 5 min. Reprinted, with permission, from Ronan et al. (2016).

morphology (10/27; 37%). Scanning electron microscopy (Fig. 5) was also used to complement confocal findings (Dong et al; 2013, Zhu et al. 2013; Li et al. 2015; Guo et al. 2017; Dong et al. 2018; Zhou et al. 2018). For transmission microscopy, sample preparation of biofilms required removal from culture plate; thus, the biofilms were mechanically scraped, which could alter cellular structure (Hu et al., 2018b).

Genetic testing was performed in 7 studies, using the polymerase chain reaction (PCR) method (Han et al. 2005, 2007; Tandiono et al. 2012; Zhu et al. 2013; Li et al. 2015; Yi et al. 2016; Dong et al. 2017; Zhou et al. 2018). PCR was used to investigate the impact of sonobactericide on (i) the expression of genes (Zhu et al. 2013; Li et al. 2015; Dong et al. 2017; Zhou et al. 2018) and mRNA (Yi et al. 2016); (ii) the successful incorporation of a gene (Han et al. 2005, 2007); and (iii) the status of genes up- and downstream after incorporation (Han et al. 2005). PCR was also used to quantify intracellular DNA released into the supernatant after treatment, which provided an indication of disrupted (lysed) cells (Tandiono et al. 2012). With respect to its advantages, PCR is not technically demanding and is fast and highly sensitive. High sensitivity is also a disadvantage concerning contamination; in addition, the specific target of interest must already be known, and caution should be taken in interpreting the results because of the potential for extracellular DNA released from bacteria not triggered by lysis. Two studies investigating intracellularly infected mammalian cells evaluated cytotoxicity in response to therapy using a trypan blue exclusion test (Ikeda-Dantsuji et al. 2011) and a lactate dehydrogenase assay (Horsley et al. 2019).

Changes in biofilm metabolism, in response to different treatments, were measured by confocal imaging with 5-cyano-2,3-ditolyltetrazolium chloride dye (Hu et al., 2018b), a CO_2-evolution monitoring system (Ronan et al. 2016) or an absorbance-based resazurin

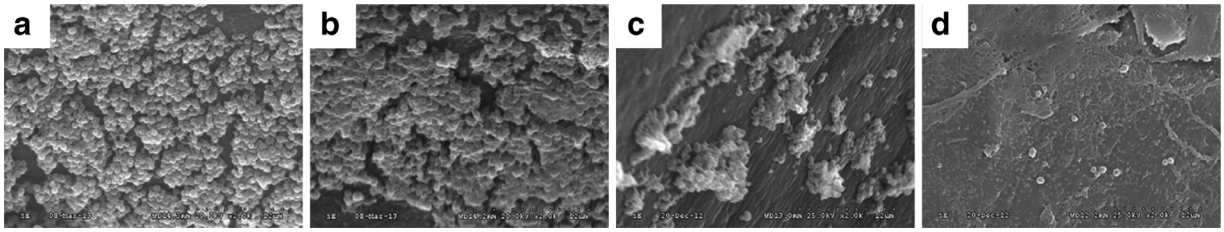

Fig. 5. Scanning electron micrographs of *Staphylococcus epidermidis* biofilms from catheters subcutaneously implanted in rabbits after treatment with (a) nothing (control); (b) ultrasound and custom-made microbubbles; (c) vancomycin (antibiotic) alone; and (d) vancomycin, ultrasound and custom-made microbubbles. Original magnification: × 2000). Ultrasound parameters were 0.3 MHz and 0.5 W/cm^2 (or 0.12 MPa) with a 50% duty cycle for a total of 20 min (5 min twice daily) Adapted, with permission, from Dong et al. (2018).

assay (Guo et al. 2017; Fu et al. 2019). Although investigation of cellular metabolism provides an indication of the overall bio-effect, the growth rate, biomass, cell viability and persister development could not be specified. Vollmer et al. (1998) and Yi et al. (2016) used bioluminescence as an indicator of bacterial cell stress responses and the distribution of stem cells in rats, respectively. Besides using fluorophore internalization, one group used a fluorescence polarization immunoassay to determine the amount of vancomycin eluted from bone cement after *in vitro* treatments (Lin et al. 2015). An enzyme-linked immunosorbent assay was also used after treatments to determine levels of gentamicin (Sugiyama et al. 2018) and inflammatory cytokines (Yi et al. 2016) in tissue. Both immunoassays are highly specific, even in samples with protein content such as serum (Yu et al. 2010; Odekerken et al. 2015), and are commercially available for various antibiotics on the market.

CAVITATION NUCLEI FOR SONOBACTERICIDE

Cavitation nuclei are a key part of sonobactericide because their volumetric changes in response to an ultrasound field induce bio-effects. From the commercially available cavitation nuclei, SonoVue was used most often (8 studies, 30%). SonoVue (available as Lumason in the United States, approved by the U.S. Food and Drug Administration [FDA] in 2016) consists of SF_6 gas microbubbles (mean diameter: 1.5−2.5 μm, ≥99% of microbubbles ≤10 μm) stabilized by a lipid coating (Schneider et al. 1995). SonoVue/Lumason is approved for clinical diagnostic use in several countries worldwide (Nolsoe and Lorentzen 2016). Other commercially available lipid-coated microbubbles have also been used for sonobactericide studies, namely, Definity (4 studies, 15%, (octafluoropropane (C_3F_8) gas core; mean diameter 1.1−3.3 μm; 98% of microbubbles <10 μm) (Definity 2011) and Sonazoid (1 study, 4%, C_4F_{10} gas core; mean diameter 2.1 μm± 0.1; <0.1% of microbubbles larger than 7 μm) (Sontum 2008). Definity and Sonazoid are approved for clinical diagnostic use in several countries worldwide (Nolsoe and Lorentzen 2016). Note that Albunex, used by Vollmer et al. (1998), was the first commercially available ultrasound contrast agent (in 1992), with a mean microbubble diameter of 3.8 μm (98.8% of microbubbles <10 μm), an air core and a human albumin coating (Feinstein 1989). However, Albunex is no longer available (Mayer and Grayburn 2001). Optison is another human albumin-coated microbubble (C_3F_8 gas core, mean diameter: 3.0−4.5 μm; 95% of microbubbles <10 μm; FDA approved in 2012) and approved for clinical use in the United States and Europe. Vollmer et al. (1998) also used custom-made microbubbles (ST68, mean diameter: 3.8 μm, air core, coating mixture of surfactants Span 60 and Tween 80 [Forsberg et al. 1997]) in their study.

The advantage of using commercially available cavitation nuclei is that their response to ultrasound has been thoroughly characterized (Gorce et al. 2000; Moran et al. 2002; Chen et al. 2003; Chetty et al. 2008; Guidi et al. 2010; Faez et al. 2011; Helfield and Goertz 2013). In addition, these cavitation nuclei are sterile with minimal batch-to-batch variability. On the other hand, custom-made cavitation nuclei as used in 11 of the sonobactericide studies can offer advantages, such as targeting by incorporating a ligand in the coating and drug loading.

Although there are several types of targeted microbubbles for ultrasound molecular imaging and drug-loaded microbubbles for ultrasound-mediated drug delivery, or a combination thereof (Sutton et al. 2013; Kooiman et al. 2014; van Rooij et al. 2015), so far only one study has employed microbubbles targeted to *S. aureus* biofilms *in vitro* using a monoclonal immunoglobulin antibody to protein A or a lectin from *P. aeruginosa* for ultrasound molecular imaging (Anastasiadis et al. 2014). These targeted microbubbles were found to bind to the biofilm matrix in proportion to the surface area.

A few studies have reported on drug-loaded microbubbles or droplets for treatment of bacterial biofilms. Horsley et al. (2019) conjugated custom-made gentamicin-loaded liposomes onto microbubbles (ratio 1:5) using biotin−avidin bridging (mean diameter: 5.79 ± 1.53 μm). The microbubbles had a gas core of SF_6 and the lipid coating consisted of 1,2-distearoyl-*sn*-glycero-3-phosphocholine (DSPC), 1,2-distearoyl-*sn*-glycero-3-phosphoethanolamine-*N*-carboxy(poly-ethylene glycol) (DSPE-PEG(2000)), DSPE-PEG-biotin and 1,2-dipalmitoyl-*sn*-glycero-3-phosphoethanolamine-*N*-(lissamine rhodamine B sulfonyl) (ammonium salt) (Rod-PE) in a molar ratio of 79.5:10:10:0.5. The protein lysozyme was used as the drug and also formed the coating of microbubbles. One study custom-made these microbubbles with an air gas core (mean diameter of 4 ± 1 or 6 ± 2 μm, depending on the duration of protein denaturation: 15 and 2 min, respectively) (Cavalieri et al. 2008; Zhou et al. 2012), and another used C_3F_8 (mean diameter: 2.5−2.9 μm, depending on the sonication power) (Liao et al. 2017). Lysozyme-coated microbubbles loaded with either spherical bovine serum albumin-coated gold nanoparticles (4.5 nm in diameter) or polyvinylpyrrolidone-coated gold nanoparticles (15 nm in diameter) were also produced by Cavalieri et al. (2013). Both types of gold nanoparticles had no effect on microbubble size distribution or stability. Mahalingam et al. (2015) produced poly (vinyl alcohol)-lysozyme-coated microbubbles (10−250 μm, nitrogen gas core) loaded with gold nanoparticles (average diameter: ∼10 nm). These microbubbles were

more stable when they contained gold nanoparticles than without them, which is in contrast to what Cavalieri et al. (2013) found. The difference in the type of coating or microbubble size could be the reason for the difference in stability.

Nanodroplets that can be phase-transitioned into microbubbles using ultrasound, a phenomenon known as acoustic droplet vaporization (Kripfgans et al. 2000; Lin and Pitt 2013), have been loaded with the antibiotic vancomycin by Argenziano et al. (2017). The nanodroplets (average diameter ~300 nm) had a core of perfluoropentane and shell of lipid and dextran sulfate to which the vancomycin was coupled by electrostatic interaction. The authors sterilized their formulation using ultraviolet light. The nanodroplets (mean diameter: 309 nm) made by Guo et al. (2017) consisted of a core of perfluoropentane and a coating of lipids. Microbubbles (mean diameter: 1.5 μm) containing a C_3F_8 gas core and coating of the same lipids were also produced.

Four groups produced custom microbubbles for co-administration with an antibiotic (Ikeda-Dantsuji et al. 2011; Dong et al. 2013, 2017, 2018), an antibiotic encapsulated in a liposome (Fu et al. 2019) or stem cells (Yi et al. 2016). Dong et al. (2013, 2017, 2018) produced lipid-coated microbubbles with a gas core of C_3F_8 and diameter of 4−6 μm. The coating consisted of the lipids DSPC and 1,2-dipalmitoyl-*sn*-glycerol-3-phosphate-ethanolamine at a molar ratio of 66:34. The microbubbles were sterilized by ^{60}Co irradiation. Ikeda-Dantsuji et al. (2011) produced microbubbles (~1 μm) encapsulating C_3F_8 gas and coated with DSPC and DSPE-PEG(2000), at a molar ratio of 94:6. Microbubbles (mean diameter: 2.39 ± 0.05 μm) with a coating of 1,2−dipalmitoyl−*sn*−glycero−3−phosphocholine, DSPE and cholesterol, mass ratio of 10:4:1 and a C_3 F_8 gas core were produced by Fu et al. (2019). A thorough characterization of the response of these microbubbles to ultrasound was not reported in these publications. The lipid-coated microbubbles (1,2-dipalmitoyl-*sn*-glycero-3-phosphoglycerol, DSPC and PEG4000 at a mass ratio of 30:30:3000 w/w) with a C_3F_8 gas core (mean: 2 μm) made by Yi et al. (2016) were compared with SonoVue for liver imaging (Liu et al. 2011). Enhancement was similar but persisted longer (still present 6 min 30 s after injection) for these custom-made microbubbles.

In the study by Halford et al. (2012), microbubbles were produced during ultrasound treatment (28−36 kHz) from a solution containing perfluorodecahydronaphthalene as oxygen carrier; 30% hydrogen peroxide, or H_2 O_2, as oxidizer; and the non-ionic detergent surfactant Triton X-100 as shell stabilizer. The figure of the formed microbubbles indicates microbubble diameters on the order of 200 μm. Non-coated microbubbles were also produced during ultrasound treatment (130 kHz) in the study by Tandiono et al. (2012). In another study, non-coated microbubbles with a mean size of 5−10 μm were produced with a microbubble generator (Agarwal et al. 2014). No specifics on the gas core and microbubble coating were provided.

The synergy between microbubbles and ultrasound exposure parameters is important for sonobactericide because the radial pulsation of microbubbles may increase the "footprint" of bactericidal action and reduce treatment times. The oscillation of each microbubble depends highly on its resonance behavior, that is, the ultrasound frequency at which the amplitude of oscillation is largest. In general, the resonance frequency is inversely related to the microbubble diameter, but the properties of the microbubble coating also play a role as rigid microbubble coatings increase the resonance frequency (Leighton 1994; Kooiman et al. 2014). Interestingly, 78% (21/27) of sonobactericide studies used lipid-coated microbubbles (see Table 1). A small fraction of the commercially available microbubbles are resonant for a particular insonification scheme because of the polydisperse population (Hettiarachchi et al. 2007). Different ultrasound center frequencies were used for sonobactericide, including frequencies used in clinical diagnostic imaging (1 MHz, 13 studies, and 1.3 MHz, 1 study; see Table 1). At these frequencies, only a subpopulation of the microbubbles are expected to oscillate in resonant modes. The ultrasound frequency employed in the other studies was lower, namely, 500 kHz (1 study), on the order of 300 kHz (4 studies), 120−130 kHz (2 studies) or between 28 and 80 kHz (7 studies). For these very low ultrasound frequencies, only microbubbles substantially larger than 10 μm in diameter would have been at resonance. Gas from the microbubbles was likely liberated and coalesced and grew by rectified diffusion in the acoustic field until the microbubbles reached resonant size (Postema et al. 2002; Bader et al. 2015). Another important consideration for microbubble oscillation is the viscosity of the surrounding medium and confinement because oscillations are damped when the viscosity increases or when microbubbles are confined (Kooiman et al. 2014). For the *in vivo* studies, the microbubbles were confined in tissue as a result of injection into the area of the implanted catheter (Dong et al. 2018), dish (He et al. 2011), titanium plate (Li et al. 2015) or tibial canal (Lin et al. 2015). It appears that these studies did not consider the effect of attenuation of ultrasound by overlying tissue.

EXPERIMENTAL OUTCOMES

All sonobactericide studies have reported an enhanced effect beyond that of antibiotics alone. The goal of all of these studies was proof-of-principle and the approaches used generally differed. Directly

comparing these 27 articles is difficult because of the large variability between them. Differences between the groups include the bacteria used and the different growth conditions, ultrasound parameters, cavitation nuclei and experimental setups. Nevertheless, this section aims to provide a discussion and make general comparisons between the experimental outcomes.

Ultrasound interacts with tissue by heating (ter Haar 2010), radiation force (Nyborg 1953) and cavitation-based mechanisms (Dalecki 2004; ter Haar 2009). Heating and radiation force could enhance the effect of antibiotics (Hajdu et al. 2010), increasing membrane permeability (Juffermans et al. 2006) and cell detachment, respectively. Cavitation is an important mechanism for sonobactericide. Stable cavitation involves gentle oscillations of microbubbles (Bader and Holland 2013), and inertial cavitation denotes the rapid growth and rapid collapse of microbubbles (Holland and Apfel 1989). The acoustic pressure required to initiate inertial cavitation can be higher than the pressure required for stable cavitation (Bader and Holland 2013) and also depends on fluid properties and the cavitation nuclei (Apfel 1997). Inertial cavitation forms microjets (Ohl et al. 2015) that can damage or deform the biofilms (Goh et al. 2015). Administration of cavitation nuclei can reduce the cavitation threshold (Bader and Holland 2013).

When microbubbles oscillate in an ultrasound field, fluid flow is generated around the microbubbles (Elder 1959; Leighton 1994). This phenomenon is known as microstreaming. The effects of microstreaming are prominent when the oscillating bubble is located near a boundary and when it is excited at resonance (Leighton 1994). Microstreaming can cause bio-effects by promoting fluid transport and producing shear stresses on cells (Collis et al. 2010). Microbubble destruction in response to ultrasound can occur through either acoustically driven diffusion or microbubble fragmentation (Chomas et al. 2001). Fragmentation in response to ultrasound exposure is typically associated with inertial cavitation (Shi et al. 2000) and can produce mechanical bio-effects.

Table 1 indicates that the majority of sonobactericide studies used one pressure amplitude, or acoustic intensity, and one center ultrasound frequency. Four studies tested multiple pressures/intensities (Han et al. 2007; Ikeda-Dantsuji et al. 2011; Goh et al. 2015; Liao et al. 2017), and one employed two frequencies (Goh et al. 2015). Ikeda-Dantsuji et al. (2011) reported that a higher ultrasound intensity (0.44 W/cm^2) further increased sonobactericide efficacy above that of doxycycline alone by approximately three times that of the lower intensity setting (0.15 W/cm^2). However, when another antibiotic (ceftizoxime), to which *C. trachomatis* is resistant, was employed, they found that the higher ultrasound intensity only slightly improved the therapeutic efficacy further. Liao et al. (2017) found that higher-intensity insonification (2 and 3 W/cm^2) beyond 1 W/cm^2 did not further enhance sonobactericide. Han et al. (2007) also found that as the acoustic pressure increased (0.25, 0.5, >0.9 MPa), delivery of their model drug into bacteria correspondingly increased.

Other ultrasound parameters were explored, such as PRF (0−100 Hz), duty cycle (5 and 50%), concentration of cavitation nuclei (0, 3.3, 10, 33% v/v) and exposure duration (0, 10, 90, 450 s) (Han et al. 2007). An increase in efficacy was seen with corresponding increased parameters, except PRF, which had no increased effect. As desired, bacterial viability was not affected among the parameters tested by Han et al. (2007) for the creation of an recA-positive strain of *Fusobacterium nucleatum*. recA renders bacteria more sensitive to ultraviolet light and reportedly repairable sonoporation (Han et al. 2007). By using similar sonobactericide conditions also on planktonic, exponential growth phase, Gram− bacteria, albeit with *E. coli*, Vollmer et al. (1998) observed bacterial death (up to 49.7 ± 6.2%) and activation of stress-response genes.

Goh et al. (2015) used high-speed optical imaging to investigate the impact of cavitating microbubbles on biofilm surfaces. At 0.1 MPa (1 MHz, 50-μs pulse), microbubble oscillation was reported to be small, and caused minimal biofilm disruption. At a higher pressure (0.7 MPa, 1 MHz, 50-μs pulse), a 7.4-μm SonoVue microbubble had an extremely large radial excursion (R_{max} = 27.3 μm) with a liquid jet within that led to mechanical dislodgement of the bacteria from the biofilm. The direction of a jet with respect to the surface of the biofilm depends on the elasticity of the surface (Ohl et al. 2015). Accordingly, jet formation can create substantial shear force leading to either an indentation or an invagination of the surface (Chen et al. 2011, 2012). Although Goh et al. (2015) used two ultrasound frequencies (0.25 and 1 MHz), they applied each frequency in a different setup (biofilm horizontally or vertically positioned). Therefore, the effects of the different frequencies could not be compared. They found that ultrasound parameters and the distance between the biofilm surface and the cavitating microbubbles affected the efficacy of biofilm disruption. Ultrasound alone did not disrupt the biofilm structure. As the initial distance between the microbubble and the biofilm increased, the disruption efficacy decreased. This observation provides support for the use of biofilm-targeted microbubbles to increase the efficacy of sonobactericide.

Ronan et al. (2016) also described biofilm disruption, in the form of craters, after ultrasound and microbubble exposure without antibiotics (Fig. 4). If bacteria are forcibly released from biofilms by microbubble oscillations, as suggested by several studies including Ronan

et al. (2016) and Goh et al. (2015), then the viability and status of these dispersed cells after treatment need to be assessed. Sonobactericide could be combined with current "traditional" or other new antimicrobials to reduce the spread of or eliminate altogether transitional dispersed cells that may be more virulent. Planktonic bacteria are often sensitive to antibiotics at much lower concentrations than are the same bacteria in biofilms (Olson et al. 2002). Thus, liberation of bacteria into the bloodstream after sonobactericide is not necessarily anticipated to pose additional risks.

Inertial cavitation caused by ultrasound-mediated microbubble destruction can produce defects in the biofilm matrix, aiding the penetration of antibiotics (He et al. 2011). Microbubbles and ultrasound exposure have been reported to increase the elution of an antibiotic from polymethylmethacrylate cement and increase the efficacy of bactericidal treatment *in vitro* and *in vivo* (Lin et al. 2015). Ultrasound-mediated microbubble destruction can also increase the metabolic activity of the bacteria in the biofilm, making it responsive to treatment with antibiotics (Hu et al., 2018b). However, Ronan et al. (2016) reported a decrease in biofilm metabolism, by analyzing carbon dioxide production, after either antibiotic alone or antibiotic combined with ultrasound and microbubbles. Because of the experimental setup, it could not be definitively determined if the decrease was from growth rate or biofilm mass reduction, and is speculated to be both. Although bacteria can develop resistance to antimicrobials over time through genetic alterations, ultrasound acts without allowing these organisms to adapt to the physical stresses (Vollmer et al. 1998). Additionally, Zhou et al. (2018) found *in vivo* that expression of the MecA gene responsible for encoding resistance to β-lactam antibiotics in MRSA was significantly reduced in the sonobactericide group with human β-defensin 3, more than twice that of the antimicrobial alone.

It has been postulated that bacterial cells could be more susceptible to sonobactericide because of their rigid cell membranes, which contrasts with the compliant phospholipid bilayers of mammalian cells that may resist rupture owing to ultrasound exposure (Conner-Kerr et al. 2010). When ultrasound is combined with cavitation nuclei and an antibiotic, sonobactericide efficacy can be enhanced, as illustrated by the *in vitro* and *in vivo* studies in this review. For example, *in vitro* studies reported by Dong et al. (2013) utilized Sonovue and reduced colony-forming units of *S. epidermidis* eightfold relative to treatment with vancomycin and ultrasound (1-MHz frequency, 0.5-W/cm^2 intensity, 50% duty cycle, 5 min). In *in vivo* studies, findings of enhanced bacterial killing when sonobactericide included an antimicrobial were also reported; for example, Sugiyama et al. (2018) observed an almost 1-log reduction in colony-forming units compared with all controls. Sonobactericide could produce equivalent therapeutic effects at a lower antibiotic dose, which may reduce complications associated with systemic toxicity, especially renal and liver complications. Sonobactericide may increase antibiotic (and other therapeutics) cytotoxicity; Horsley et al. (2019) reported higher toxicity in human urothelial cells with ultrasound-exposed solutions of microbubbles coated with liposomes containing gentamicin at 2.64 and 5.28 μg/mL than free gentamicin at the much higher clinically approved dosage (200 μg/mL). This finding highlights that cytotoxicity should be more widely considered as a sonobactericide test parameter in future studies.

In addition to Han et al. (2007), the microbubble dose dependence of sonobactericide has been investigated by three other groups that found an increase in the efficacy of sonobactericide with increasing concentration of microbubbles (Ikeda-Dantsuji et al. 2011; Dong et al. 2013, 2017), indicating dose-dependent synergy. Only Han et al. (2007) used more than two concentrations, with which a near-linear trend between microbubble concentration and treatment efficacy could be observed. A similar increase in bio-effects with increasing microbubble concentration has been reported for sonoporation of eukaryotic cells (Ward et al. 2000) and blood−brain barrier disruption (Song et al. 2017). Increasing the antibiotic concentration also resulted in an increasing dose−effect relationship for all treatments of *Acinetobacter baumannii*, including microbubbles combined with free polymyxin B and microbubbles combined with free chitosan-modified polymyxin B-loaded liposomes (Fu et al. 2019). Horsley et al. (2019) increased both antibiotic and microbubble concentrations, because gentamicin was encapsulated on liposomes bound to the microbubbles, which led to an enhanced reduction of bacterial load in infected urothelial cells.

The "in vial" concentration of Definity is 4.2×10^9 microbubbles/mL, that of Albunex 7×10^8 microbubbles/mL (Christiansen et al. 1994) and that of SonoVue/Lumason 3.0×10^8 to 1.1×10^9 microbubbles/mL. Assuming a blood volume of 5 L in an average human, the *in vivo* concentrations for Definity, Albunex and Lumason correspond to 8.4×10^5/mL, 1.4×10^5/mL and 6×10^4 to 2.2×10^5/mL, respectively. Several sonobactericide studies reported thus far have used high concentrations of microbubbles (10^7 to 10^8/mL) both *in vitro* (Vollmer et al. 1998; Dong et al. 2013, 2017; Hu et al., 2018b) and *in vivo* (He et al. 2011; Li et al. 2015; Dong et al. 2018), relative to the concentrations currently used in clinical diagnostic imaging. This approach could potentially be employed in non-vascular applications such as dental, skin wound and implant biofilms (He et al. 2011, Li et al. 2015, Dong et al. 2018).

Furthermore, pre-clinical studies in both small animal and rodent models suggest that high concentrations of microbubbles administered intravenously, up to 250 times higher than the clinical dose, may be well tolerated (Schneider et al. 2011). Although *in vitro* studies have indicated that large microbubbles (~0.3 mm) can destroy biofilms under flow by microbubble collision (Sharma et al. 2005; Parini and Pitt 2006), this mechanism is unlikely to occur for microbubbles of clinically relevant sizes for vascular applications (*i.e.,* 1−10 μm).

Five studies used custom-made lysozyme-coated microbubbles in the absence of ultrasound (Cavalieri et al. 2008, 2012; Zhou et al. 2012; Cavalieri et al. 2013; Mahalingam et al. 2015). These exhibited antimicrobial properties on *Micrococcus lysodeikticus, S. aureus* and *E. coli.* Lysozyme-coated microbubbles, or poly(vinyl alcohol)-lysozyme-coated microbubbles, loaded with gold nanoparticles were found to have a stronger antimicrobial effect than non-loaded microbubbles on planktonic *Micrococcus lysodeikticus* (Cavalieri et al. 2013) and *E. coli* (Mahalingam et al. 2015). The coated gold nanoparticles alone lacked lytic activity in the Cavalieri study, and thus the authors attributed the enhanced antimicrobial effect of the gold nanoparticles loaded on the lysozyme microbubbles to improved binding and, consequently, increased interaction of the bacteria with the surface of the lysozyme-microbubbles. Contrarily, gold nanoparticles alone had an antibacterial rate of ~50% at 3 h in the Mahalingam et al. (2015) study. The difference in antibacterial activity of gold nanoparticles could be explained by the different bacteria employed. Combining these lysozyme-coated microbubbles with ultrasound could have further enhanced the antimicrobial properties as Liao et al. (2017) observed when using them in their *in vitro* and *in vivo* study. Sonobactericide used against *P. acnes* had an enhanced antibacterial effect and resulted in a 1.45-fold reduction in inflammatory reactions relative to lysozyme-coated microbubbles alone. Furthermore, after 13 d of treatment, inflammation was no longer observed.

Vancomycin-loaded nanodroplets (Argenziano et al. 2017), in the absence of ultrasound, were significantly more effective at an earlier time point than vancomycin alone or non-loaded nanodroplets alone in killing planktonic MRSA (isolated from human ulcerated wounds). The authors attributed their findings to the time-sustained release of vancomycin from the loaded nanodroplets. However, the altered charge could also have played a role as vancomycin is positively charged and the vancomycin-loaded nanodroplets are negatively charged. Ultrasound exposure significantly enhanced vancomycin delivery from the loaded nanodroplets *ex vivo* through non-infected porcine skin, indicating the potential to treat skin infections (Argenziano et al. 2017).

CLINICAL TRANSLATION OF SONOBACTERICIDE

Diagnostic ultrasound contrast examinations are performed worldwide (Madsen and Rasmussen 2011; Wei 2012; Alzaraa et al. 2013; Nolsoe and Lorentzen 2016), including for the detection of the metastatic spread of bacterial infective endocarditis (Menozzi et al. 2013a, 2013b). Fifteen of the 27 sonobactericide studies (56%) used microbubbles that are clinically approved, by the FDA and European Medicines Agency, which could help with the translation of sonobactericide into the clinic. Contrarily, sonobactericide with custom-made microbubbles containing Triton (Halford et al. 2012) is not translatable because this surfactant is toxic to cells (Jahan et al. 2008; Koley and Bard 2010). The ideal characteristics of a clinically relevant treatment can be broadly described as improved patient outcomes, reduction in treatment times and practical implementation in the clinic. More specifically, broad-spectrum bactericidal activity, low risk for inducing resistance and minimal mammalian cell cytotoxicity could be considered. The reader is referred to two review articles that provide conceptional discussions on the ideal antibiotic that could aid sonobactericide strategies (Lewis 2013, Gajdács 2019). The use of clinically relevant animal models of biofilm would help translate the development of sonobactericide. For example, Lin et al. (2015) used a periprosthetic infection rabbit tibia model. However, periprosthetic joint infection models have limited translational value as described in the review by Carli et al. (2016). While proposing criteria for an optimal animal model, this review stresses the critical importance of animal, pathogen, implant and outcome measurement selection and a method that replicates the "human" periprosthetic environment, wherein at least one of these areas current models fall short.

The choice of ultrasound insonification parameters is important for the clinical translation of sonobactericide. A wide frequency range (tens of kilohertz to 1.3 MHz) has been reported for sonobactericide (see Table 1), along with pulsed (Vollmer et al. 1998; Lin et al. 2015; Horsley et al. 2019), continuous wave (Zhu et al. 2013; Fu et al. 2019) or intermittent (Agarwal et al. 2014; Lattwein et al. 2018) ultrasound in sonification. More studies directly investigating different ultrasound parameters should be performed to better understand the effect they have on sonobactericide. The choice of frequency and exposure parameters needs to focus on safety, efficacy and compatibility with existing clinical workflows for rapid clinical translation. Several *in vitro* studies have been conducted in sonication baths at frequencies ranging from 20−80 kHz (Zhu et al. 2013, 2014), which are likely not directly suitable for *in vivo*

applications. Physiotherapy probes (He et al. 2011; Li et al. 2015; Hu et al., 2018b) and gene transfer equipment (Dong et al. 2013, 2017; Fu et al. 2019) have also been adapted for sonobactericide studies. Development of specialized probes may be necessary for treating biofilms that are not easily accessible or where a small geometric footprint may be needed. Ultrasonic energy may be delivered to infected areas either extracorporeally or using catheter-based ultrasound probes. Catheters have been reported previously for sonothrombolysis (Owens 2008; Kim et al. 2017), and could be investigated for sonobactericide in vascular organs.

Microbubble concentration, type and route depend on the location of the biofilm being treated. Microbubbles can be delivered intravenously, intra-arterially or by direct injection into the site of interest (Goldberg et al. 1994). When necessary, high concentrations can be achieved site-specifically by local infusion of microbubbles. On the other hand, delivering microbubbles to biofilm infections associated with prosthetic joints may be challenging because the biofilm is typically located within the joint space (McConoughey et al. 2014). In the case of bacterial infective endocarditis, contact between the microbubbles and the biofilm may be hampered by rapid pulsatile blood flow. Targeting the microbubbles to the biofilm could further aid in therapeutic efficacy. Clinical phase 0 trials have successfully been completed for ultrasound molecular imaging of prostate, ovarian and breast cancer using targeted microbubbles (Smeenge et al. 2017; Willmann et al. 2017), thereby paving the way for clinical use of targeted microbubbles. The *S. aureus* biofilm-targeted microbubbles developed by Anastasiadis et al. (2014) lack clinical translation because the *P. aeruginosa* lectin used as ligand causes red blood cell agglutination (Gilboa-Garber and Sudakevitz 1999), and the protein A antibody used as ligand must compete with host antibodies that cover protein A (Bröker et al. 2014). For other potential targeting possibilities, the reader is referred to the reviews by van Oosten et al. (2015) and Koo et al. (2017).

CONCLUSIONS AND FUTURE PERSPECTIVES

Therapeutic effects of sonobactericide can include direct bacterial killing, biofilm degradation and dispersal and increased or synergistic therapeutic effectiveness of antimicrobials or other drugs, all resulting from the physical phenomena of ultrasound combined with cavitation nuclei aided by the addition of an antimicrobial agent. It is the different time scales at which these actions occur that makes sonobactericide challenging, as illustrated in Figure 6. The time scale of the microbubble vibration is on the order of microseconds in a megahertz ultrasound field, which is many orders of magnitude smaller than the time scale of physiologic effects (milliseconds), let alone that of biological effects (seconds to minutes) and clinical relevance (days to months). The link between, and the mechanistic aspects of, cavitation nucleation, the effect on (intracellular) bacteria/biofilms and antimicrobial drug release and uptake need to be elucidated in future studies to efficiently treat bacterial infections.

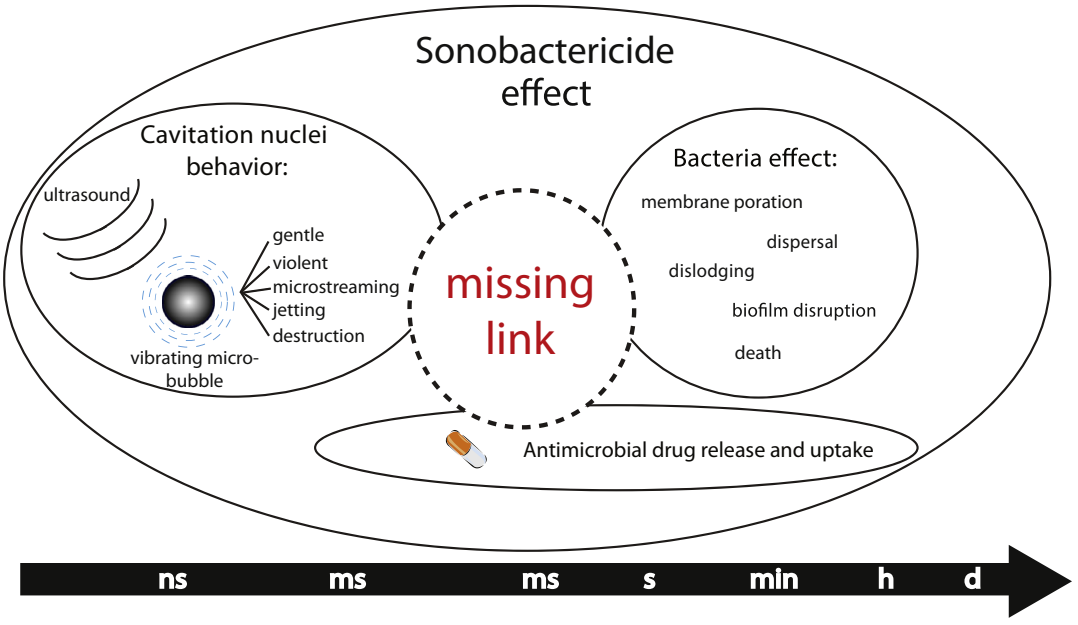

Fig. 6. Different time scales of the therapeutic effects of sonobactericide.

The effect of the biofilm type on sonobactericide efficacy has received limited attention. For example, the age and composition of the biofilm (Shen et al. 2010) may contribute to its resilience to sonobactericide. The antibiotic penetration through biofilm decreases appreciably with the age of the biofilm (Carmen et al. 2004). Additionally, biofilms formed *in vivo* may differ in composition and morphology from *in vitro* biofilm models (Bjarnsholt et al. 2013). For example, recent research has indicated that infective endocarditis can be a polymicrobial infection (Oberbach et al. 2017). These effects should be elucidated in future pre-clinical and clinical studies, as also addressed in other reviews (Coenye and Nelis 2010, Malone et al. 2017).

Nanoscale cavitation nucleating agents such as nanodroplets and polymeric nanocups (Kwan et al. 2015) could be interesting for sonobactericide as they could penetrate the biofilm and help nucleate cavitation throughout the biofilm. In particular, the process of droplet vaporization may exert mechanical forces on the biofilm in addition to antibiotic activity (Guo et al. 2017). Nanodroplets can nucleate sustained cavitation in closed fluid spaces (Chen et al. 2013). Polymeric nanocups nucleate inertial cavitation activity with thresholds inversely proportional to size. For example, nanocups with mean sizes of 180 and 600 nm have been reported to nucleate inertial cavitation at peak rarefactional pressures of 3 and 0.5 MPa, respectively (Kwan et al. 2015). These agents have not yet been investigated for treating biofilms. Despite the potential advantages offered by nanodroplets and nanocups, these agents are not yet clinically approved or readily available. Therefore, sonobactericide using these agents may not be clinically feasible in the near future.

Recalcitrant biofilms may be treated with shock waves (Gnanadhas et al. 2015; Qi et al. 2016) or histotripsy (Xu et al. 2012; Bigelow et al. 2017). Jetting from shock waves has been used in the clinic to destroy kidney stones and gallstones with lithotripsy (Vakil and Everbach 1993). Highly focused image-guided ultrasound beams can help concentrate acoustic energy at the biofilm site, while avoiding collateral damage. Histotripsy can be combined with a cavitation nucleation agent, such as phase-shift nanodroplets (Vlaisavljevich et al. 2013) and echogenic liposomes (Bader et al. 2016b), to lower the acoustic pressure thresholds for ablation, which could potentially improve the safety profile of treatment. Another potential application to treat biofilm infections harnessing sound is an ultrasonically activated stream. Birkin et al. (2015) reported that by applying low-amplitude ultrasound (135 kHz, 120−250 kPa) through a liquid stream directed at a surface, endogenous cavitation nuclei can be sufficiently activated at the solid/liquid interface to disrupt biofilm.

Combining ultrasound, cavitation nuclei and antibiotic therapy with matrix-degrading enzymes implicated in biofilm dispersal, such as glycosidases, proteases and deoxyribonucleases (Kaplan 2010; Zhu et al. 2013; Li et al. 2015), is a promising strategy for treating biofilms. Our group has recently reported the use of rtPA, a clinically approved fibrinolytic agent, along with Definity microbubbles, an antibiotic and 120-kHz intermittent ultrasound for sonobactericide in an *in vitro* flow model (Lattwein et al. 2018). This strategy could be promising for treating biofilms that have fibrin as a primary structural component. The microstreaming produced by cavitation nuclei (Kooiman et al. 2014) can help remove biofilm degradation products and enhance the delivery of drugs, similar to sonothrombolysis studies (Bader et al. 2016a). Although the feasibility of biofilm dispersal has been reported in previous studies (Kaplan 2010), more work needs to be done to elucidate the efficacy of combination therapy with matrix-degrading enzymes, ultrasound and microbubbles. Future research could also include the interference of quorum sensing, which is bacterial communication that regulates several virulence pathways through signaling molecules and increases with cell density (Whiteley et al. 2017). Because of the high potential of this approach, many compounds are under development that could be combined with sonobactericide to enhance efficacy (Fleitas Martínez et al. 2019). In addition, it is unknown if sonobactericide has an effect on quorum sensing without these agents.

The safety and efficacy of sonobactericide are paramount. Accurate characterization of the acoustic fields (ter Haar et al. 2011) and parameters used, standardization of protocols for the assessment of treatment efficacy and development of *in vitro* and pre-clinical models that mimic the *in vivo* milieu will help accelerate the transition of sonobactericide to the clinic. In addition, enabling image guidance methods, such as active (Miller et al. 2016) or passive cavitation imaging (Haworth et al. 2017) and real-time feedback (Sun et al. 2017), may help monitor treatment progress, standardize the acoustic dose and aid in improving the safety and efficacy of *in situ* destruction of biofilms.

Acknowledgments—Financial support from the Erasmus MC Foundation (fellowship to K.K.) and U.S. National Institutes of Health, National Institute of Neurologic Disorders and Stroke, Grant R01 NS047603 (PI: C.K.H.) is gratefully acknowledged. The Erasmus MC Foundation is the funding agency for the fellowship to Klazina Kooiman.

Conflict of interest disclosure—The authors declare no competing interests.

REFERENCES

Agarwal A, Jern Ng W, Liu Y. Removal of biofilms by intermittent low-intensity ultrasonication triggered bursting of microbubbles. Biofouling 2014;30:359–365.

Algburi A, Comito N, Kashtanov D, Dicks LMT, Chikindas ML. Control of biofilm formation: Antibiotics and beyond. Appl Environ Microbiol 2017;83 pii: e02508−16.

Alzaraa A, Gravante G, Chung WY, Al-Leswas D, Morgan B, Dennison A, Lloyd D. Contrast-enhanced ultrasound in the preoperative, intraoperative and postoperative assessment of liver lesions. Hepatol Res 2013;43:809–819.

Anastasiadis P, Mojica KD, Allen JS, Matter ML. Detection and quantification of bacterial biofilms combining high-frequency acoustic microscopy and targeted lipid microparticles. J Nanobiotechnol 2014;12:24.

Apfel RE. Sonic effervescence: A tutorial on acoustic cavitation. J Acoust Soc Am 1997;101:1227–1237.

Archer NK, Mazaitis MJ, Costerton JW, Leid JG, Powers ME, Shirtliff ME. *Staphylococcus aureus* biofilms: Properties, regulation, and roles in human disease. Virulence 2011;2:445–459.

Argenziano M, Banche G, Luganini A, Finesso N, Allizond V, Gulino GR, Khadjavi A, Spagnolo R, Tullio V, Giribaldi G, Guiot C, Cuffini AM, Prato M, Cavalli R. Vancomycin-loaded nanobubbles: A new platform for controlled antibiotic delivery against methicillin-resistant *Staphylococcus aureus* infections. Int J Pharm 2017;523:176–188.

Azuma T, Kawabata KI, Umemura SI, Ogihara M, Kubota J, Sasaki A, Furuhata H. Bubble generation by standing wave in water surrounded by cranium with transcranial ultrasonic beam. Japan J Appl Phys 2005;44:4625–4630.

Baddour LM, Wilson WR, Bayer AS, Fowler VG, Jr, Tleyjeh IM, Rybak MJ, Barsic B, Lockhart PB, Gewitz MH, Levison ME, Bolger AF, Steckelberg JM, Baltimore RS, Fink AM, O'Gara P, Taubert KA. American Heart Association Committee on Rheumatic Fever, Endocarditis, and Kawasaki Disease of the Council on Cardiovascular Disease in the Young; Council on Clinical Cardiology; Council on Cardiovascular Surgery and Anesthesia; and Stroke Council. Infective endocarditis in adults: Diagnosis, antimicrobial therapy, and management of complications: A scientific statement for healthcare professionals from the American Heart Association. Circulation 2015;132:1435–1486.

Bader KB, Holland CK. Gauging the likelihood of stable cavitation from ultrasound contrast agents. Phys Med Biol 2013;58:127–144.

Bader KB, Gruber MJ, Holland CK. Shaken and stirred: Mechanisms of ultrasound-enhanced thrombolysis. Ultrasound Med Biol 2015;41:187–196.

Bader KB, Bouchoux G, Holland CK. Sonothrombolysis. Adv Exp Med Biol 2016;880:339–362.

Bader KB, Haworth KJ, Shekhar H, Maxwell AD, Peng T, McPherson DD, Holland CK. Efficacy of histotripsy combined with rt-PA in vitro. Phys Med Biol 2016;61:5253–5274.

Bæk KT, Frees D, Renzoni A, Barras C, Rodriguez N, Manzano C, Kelley WL. Genetic variation in the *Staphylococcus aureus* 8325 strain lineage revealed by whole-genome sequencing. PloS One 2013;8:e77122.

Bigelow TA, Thomas CL, Wu H, Itani KMF. Histotripsy treatment of S. aureus biofilms on surgical mesh samples under varying pulse durations. IEEE Trans Ultrason Ferroelectr Freq Control 2017;64:1420–1428.

Birkin PR, Offin DG, Vian CJB, Howlin RP, Dawson JI, Secker TJ, Hervé RC, Stoodley P, Oreffo ROC, Keevil CW, Leighton TG. Cold water cleaning of brain proteins, biofilm and bone— Harnessing an ultrasonically activated stream. Phys Chem Chem Phys 2015;17:20574–20579.

Bjarnsholt T, Alhede M, Alhede M, Eickhardt-Sørensen SR, Moser C, Kühl M, Jensen PØ, Høiby N. The *in vivo* biofilm. Trends Microbiol 2013;21:466–474.

Black JJ, Yu FT, Schnatz RG, Chen X, Villanueva FS, Pacella JJ. Effect of thrombus composition and viscosity on sonoreperfusion efficacy in a model of micro-vascular obstruction. Ultrasound Med Biol 2016;42:2220–2231.

Brady RA, Mocca CP, Plaut RD, Takeda K, Burns DL. Comparison of the immune response during acute and chronic Staphylococcus aureus infection. PloS One 2018;13 e0195342.

Bröker BM, Holtfreter S, Bekeredjian-Ding I. Immune control of *Staphylococcus aureus*− Regulation and counter-regulation of the adaptive immune response. Int J Med Microbiol 2014;304:204–214.

Cai Y, Wang J, Liu X, Wang R, Xia L. A review of the combination therapy of low frequency ultrasound with antibiotics. BioMed Res Int 2017;2017:14.

Carli AV, Ross FP, Bhimani SJ, Nodzo SR, Bostrom MP. Developing a clinically representative model of periprosthetic joint infection. J Bone Joint Surg Am 2016;98:1666–1676.

Carmen JC, Nelson JL, Beckstead BL, Runyan CM, Robison RA, Schaalje GB, Pitt WG. Ultrasonic-enhanced gentamicin transport through colony biofilms of Pseudomonas aeruginosa and *Escherichia coli*. J Infect Chemother 2004;10:193–199.

Carugo D, Owen J, Crake C, Lee JY, Stride E. Biologically and acoustically compatible chamber for studying ultrasound-mediated delivery of therapeutic compounds. Ultrasound Med Biol 2015;41:1927–1937.

Cavalieri F, Ashokkumar M, Grieser F, Caruso F. Ultrasonic synthesis of stable, functional lysozyme microbubbles. Langmuir 2008;24:10078–10083.

Cavalieri F, Zhou M, Tortora M, Lucilla B, Ashokkumar M. Methods of preparation of multifunctional microbubbles and their in vitro/in vivo assessment of stability, functional and structural properties. Curr Pharm Des 2012;18:2135–2151.

Cavalieri F, Micheli L, Kaliappan S, Teo BM, Zhou M, Palleschi G, Ashokkumar M. Antimicrobial and biosensing ultrasound-responsive lysozyme-shelled microbubbles. ACS Appl Mater Interfaces 2013;5:464–471.

Chen WS, Matula TJ, Brayman AA, Crum LA. A comparison of the fragmentation thresholds and inertial cavitation doses of different ultrasound contrast agents. J Acoust Soc Am 2003;113:643–651.

Chen H, Kreider W, Brayman AA, Bailey MR, Matula TJ. Blood vessel deformations on microsecond time scales by ultrasonic cavitation. Phys Rev Lett 2011;106 034301.

Chen H, Brayman AA, Evan AP, Matula TJ. Preliminary observations on the spatial correlation between short-burst microbubble oscillations and vascular bioeffects. Ultrasound Med Biol 2012;38:2151–2162.

Chen CC, Sheeran PS, Wu S-Y, Olumolade OO, Dayton PA, Konofagou EE. Targeted drug delivery with focused ultrasound-induced blood−brain barrier opening using acoustically-activated nanodroplets. J Controlled Release 2013;172:795–804.

Chetty K, Stride E, Sennoga CA, Hajnal JV, Eckersley RJ. High-speed optical observations and simulation results of SonoVue microbubbles at low-pressure insonation. IEEE Trans Ultrason Ferroelectr Freq Control 2008;55:1333–1342.

Chomas JE, Dayton P, Allen J, Morgan K, Ferrara KW. Mechanisms of contrast agent destruction. IEEE Trans Ultrason Ferroelectr Freq Control 2001;48:232–248.

Christiansen C, Kryvi H, Sontum PC, Skotland T. Physical and biochemical characterization of Albunex, a new ultrasound contrast agent consisting of air-filled albumin microspheres suspended in a solution of human albumin. Biotechnol Appl Biochem 1994;19:307–320.

Chua SL, Liu Y, Yam JKH, Chen Y, Vejborg RM, Tan BGC, Kjelleberg S, Tolker-Nielsen T, Givskov M, Yang L. Dispersed cells represent a distinct stage in the transition from bacterial biofilm to planktonic lifestyles. Nat Commun 2014;5:4462.

Coakley WT, Bardsley DW, Grundy MA, Zamani F, Clarke DJ. Cell manipulation in ultrasonic standing wave fields. J Chem Technol Biotechnol 1989;44:43–62.

Coenye T, Nelis HJ. In vitro and in vivo model systems to study microbial biofilm formation. J Microbiol Methods 2010;83:89–105.

Collis J, Manasseh R, Liovic P, Tho P, Ooi A, Petkovic-Duran K, Zhu Y. Cavitation microstreaming and stress fields created by microbubbles. Ultrasonics 2010;50:273–279.

Conner-Kerr T, Alston G, Stovall A, Vernon T, Winter D, Meixner J, Grant K, Kute T. The effects of low-frequency ultrasound (35 kHz) on methicillin-resistant *Staphylococcus aureus* (MRSA) in vitro. Ostomy Wound Manag 2010;56:32–43.

Connolly KL, Roberts AL, Holder RC, Reid SD. Dispersal of group A streptococcal biofilms by the cysteine protease SpeB leads to increased disease severity in a murine model. PloS One 2011;6: e18984.

Costerton JW, Stewart PS, Greenberg EP. Bacterial biofilms: A common cause of persistent infections. Science 1999;284:1318–1322.

Crosby HA, Kwiecinski J, Horswill AR. *Staphylococcus aureus* aggregation and coagulation mechanisms, and their function in host-pathogen interactions. Adv Appl Microbiol 2016;96:1–41.

Dalecki D. Mechanical bioeffects of ultrasound. Annu Rev Biomed Eng 2004;6:229–248.

Deffieux T, Konofagou EE. Numerical study of a simple transcranial focused ultrasound system applied to blood-brain barrier opening. IEEE Trans Ultrason Ferroelectr Freq Control 2010;57:2637–2653.

Delcaru C, Alexandru I, Podgoreanu P, Grosu M, Stavropoulos E, Chifiriuc CM, Lazar V. Microbial biofilms in urinary tract infections and prostatitis: Etiology, pathogenicity, and combating strategies. Pathogens 2016;5(4):65.

Dhople V, Krukemeyer A, Ramamoorthy A. The human beta-defensin-3, an antibacterial peptide with multiple biological functions. Biochim Biophys Acta 2006;1758:1499–1512.

Dong Y, Chen S, Wang Z, Peng N, Yu J. Synergy of ultrasound microbubbles and vancomycin against *Staphylococcus epidermidis* biofilm. J Antimicrob Chemother 2013;68:816–826.

Dong Y, Xu Y, Li P, Wang C, Cao Y, Yu J. Antibiofilm effect of ultrasound combined with microbubbles against *Staphylococcus epidermidis* biofilm. Int J Med Microbiol 2017;307:321–328.

Dong Y, Li J, Li P, Yu J. Ultrasound microbubbles enhance the activity of vancomycin against *Staphylococcus epidermidis* biofilms in vivo. J Ultrasound Med 2018;37:1379–1387.

Elder SA. Cavitation microstreaming. J Acoust Soc Am 1959;31:54–64.

Erriu M, Blus C, Szmukler-Moncler S, Buogo S, Levi R, Barbato G, Madonnaripa D, Denotti G, Piras V, Orru G. Microbial biofilm modulation by ultrasound: Current concepts and controversies. Ultrason Sonochem 2014;21:15–22.

Escoffre JM, Piron J, Novell A, Bouakaz A. Doxorubicin delivery into tumor cells with ultrasound and microbubbles. Mol Pharm 2011;8:799–806.

Estrela C, Estrela CR, Barbin EL, Spano JC, Marchesan MA, Pecora JD. Mechanism of action of sodium hypochlorite. Braz Dent J 2002;13:113–117.

Faez T, Goertz D, De Jong N. Characterization of Definity ultrasound contrast agent at frequency range of 5-15 MHz. Ultrasound Med Biol 2011;37:338–342.

Feinstein SB. New developments in ultrasonic contrast techniques: Transpulmonary passage of contrast agent and diagnostic implications. Echocardiography 1989;6:27–33.

Fleitas Martínez O, Rigueiras PO, Pires ÁdS, Porto WF, Silva ON, de la Fuente-Nunez C, Franco OL. Interference with quorum-sensing signal biosynthesis as a promising therapeutic strategy against multidrug-resistant pathogens. Front Cell Infect Microbiol 2019;8:444.

Forsberg F, Wu Y, Makin IR, Wang W, Wheatley MA. Quantitative acoustic characterization of a new surfactant-based ultrasound contrast agent. Ultrasound Med Biol 1997;23:1201–1208.

Fu YY, Zhang L, Yang Y, Liu CW, He YN, Li P, Yu X. Synergistic antibacterial effect of ultrasound microbubbles combined with chitosan-modified polymyxin B-loaded liposomes on biofilm-producing *Acinetobacter baumannii*. Int J Nanomed 2019;14:1805–1815.

Fux CA, Stoodley P, Hall-Stoodley L, Costerton JW. Bacterial biofilms: A diagnostic and therapeutic challenge. Expert Rev Anti-infect Ther 2003;1:667–683.

Gajdács M. The concept of an ideal antibiotic: Implications for drug design. Molecules 2019;24:892.

Gilboa-Garber N, Sudakevitz D. The hemagglutinating activities of *Pseudomonas aeruginosa* lectins PA-IL and PA-IIL exhibit opposite temperature profiles due to different receptor types. FEMS Immunol Med Microbiol 1999;25:365–369.

Gnanadhas DP, Elango M, Janardhanraj S, Srinandan CS, Datey A, Strugnell RA, Gopalan J, Chakravortty D. Successful treatment of biofilm infections using shock waves combined with antibiotic therapy. Sci Rep 2015;5:17440. –17440.

Goh BHT, Conneely M, Kneuper H, Palmer T, Klaseboer E, Khoo BC, Campbell P. High-speed imaging of ultrasound-mediated bacterial biofilm disruption. In: Lacković I, Vasic D, (eds). Proceedings, 6th European Conference of the International Federation for Medical and Biological Enginnering. Cham. Springer; 2015;45: 533–536.

Goldberg BB, Liu JB, Forsberg F. Ultrasound contrast agents: A review. Ultrasound Med Biol 1994;20:319–333.

Gorce JM, Arditi M, Schneider M. Influence of bubble size distribution on the echogenicity of ultrasound contrast agents: A Study of SonoVue. Invest Radiol 2000;35:661–671.

Grant SS, Hung DT. Persistent bacterial infections, antibiotic tolerance, and the oxidative stress response. Virulence 2013;4:273–283.

Guidi F, Vos HJ, Mori R, Jong ND, Tortoli P. Microbubble characterization through acoustically induced deflation. IEEE Trans Ultrason Ferroelectr Freq Control 2010;57:193–202.

Guo H, Wang ZM, Du QY, Li P, Wang ZG, Wang AM. Stimulated phase-shift acoustic nanodroplets enhance vancomycin efficacy against methicillin-resistant *Staphylococcus aureus* biofilms. Int J Nanomed 2017;12:4679–4690.

Habib G, Lancellotti P, Antunes MJ, Bongiorni MG, Casalta J-P, Del Zotti F, Dulgheru R, El Khoury G, Erba PA, Iung B, Miro JM, Mulder BJ, Plonska-Gosciniak E, Price S, Roos-Hesselink J, Snygg-Martin U, Thuny F, Tornos Mas P, Vilacosta I, Zamorano JL, Group ESD. 2015 ESC guidelines for the management of infective endocarditis: The Task Force for the Management of Infective Endocarditis of the European Society of Cardiology. Eur Heart J 2015;36:3075–3128.

Hajdu S, Holinka J, Reichmann S, Hirschl AM, Graninger W, Presterl E. Increased temperature enhances the antimicrobial effects of daptomycin, vancomycin, tigecycline, fosfomycin, and cefamandole on staphylococcal biofilms. Antimicrob Agents Chemother 2010;54:4078–4084.

Halford A, Ohl CD, Azarpazhooh A, Basrani B, Friedman S, Kishen A. Synergistic effect of microbubble emulsion and sonic or ultrasonic agitation on endodontic biofilm in vitro. J Endod 2012;38:1530–1534.

Han YW, Ikegami A, Rajanna C, Kawsar HI, Zhou Y, Li M, Sojar HT, Genco RJ, Kuramitsu HK, Deng CX. Identification and characterization of a novel adhesin unique to oral fusobacteria. J Bacteriol 2005;187:5330–5340.

Han YW, Ikegami A, Chung P, Zhang L, Deng CX. Sonoporation is an efficient tool for intracellular fluorescent dextran delivery and one-step double-crossover mutant construction in *Fusobacterium nucleatum*. Appl Environ Microbiol 2007;73:3677–3683.

Haworth KJ, Bader KB, Rich KT, Holland CK, Mast TD. Quantitative frequency-domain passive cavitation imaging. IEEE Trans Ultrason Ferroelectr Freq Control 2017;64:177–191.

He N, Hu J, Liu H, Zhu T, Huang B, Wang X, Wu Y, Wang W, Qu D. Enhancement of vancomycin activity against biofilms by using ultrasound-targeted microbubble destruction. Antimicrob Agents Chemother 2011;55:5331–5337.

Helfield BL, Goertz DE. Nonlinear resonance behavior and linear shell estimates for Definity and MicroMarker assessed with acoustic microbubble spectroscopy. J Acoust Soc Am 2013;133:1158–1168.

Hensel K, Mienkina MP, Schmitz G. Analysis of ultrasound fields in cell culture wells for in vitro ultrasound therapy experiments. Ultrasound Med Biol 2011;37:2105–2115.

Hettiarachchi K, Talu E, Longo ML, Dayton PA, Lee AP. On-chip generation of microbubbles as a practical technology for manufacturing contrast agents for ultrasonic imaging. Lab Chip 2007;7:463–468.

Holland CK, Apfel RE. An improved theory for the prediction of microcavitation thresholds. IEEE Trans Ultrason Ferroelectr Freq Control 1989;36:204–208.

Horsley H, Owen J, Browning R, Carugo D, Malone-Lee J, Stride E, Rohn JL. Ultrasound-activated microbubbles as a novel intracellular drug delivery system for urinary tract infection. J Control Release 2019;301:166–175.

Hu F, Zhu D, Wang F, Wang M. Current status and trends of antibacterial resistance in China. Clin Infect Dis 2018a;67:S128–SS34.

Hu J, Zhang N, Jr, Li L, Zhang N, Sr, Ma Y, Zhao C, Wu Q, Li Y, He N, Wang X. The synergistic bactericidal effect of vancomycin on

UTMD treated biofilm involves damage to bacterial cells and enhancement of metabolic activities. Sci Rep 2018b;8:192.

Huber TM, Beaver NM, Helps JR. Elimination of standing wave effects in ultrasound radiation force excitation in air using random carrier frequency packets. J Acoust Soc Am 2011;130:1838–1843.

Ikeda-Dantsuji Y, Feril LB, Jr, Tachibana K, Ogawa K, Endo H, Harada Y, Suzuki R, Maruyama K. Synergistic effect of ultrasound and antibiotics against *Chlamydia trachomatis*-infected human epithelial cells in vitro. Ultrason Sonochem 2011;18:425–430.

Jahan K, Balzer S, Mosto P. Toxicity of nonionic surfactants. Wit Trans Ecol Environ 2008;110:281–290.

Juffermans LJ, Dijkmans PA, Musters RJ, Visser CA, Kamp O. Transient permeabilization of cell membranes by ultrasound-exposed microbubbles is related to formation of hydrogen peroxide. Am J Physiol Heart Circ Physiol 2006;291:H1595–H1601.

Kaplan JB. Biofilm dispersal: Mechanisms, clinical implications, and potential therapeutic uses. J Dent Res 2010;89:205–218.

Kim J, Lindsey BD, Chang W-Y, Dai X, Stavas JM, Dayton PA, Jiang X. Intravascular forward-looking ultrasound transducers for microbubble-mediated sonothrombolysis. Sci Rep 2017;7:3454.

Kinsler LE, Frey AR, Coppens AB, Sanders JV. Fundamentals of acoustics. New York: Wiley; 2000.

Kleven RT, Karani KB, Salido NG, Shekhar H, Haworth KJ, Mast TD, Tadessel DG, Holland CK. The effect of 220 kHz insonation scheme on rt-PA thrombolytic efficacy in vitro. Phys Med Biol 2019;64 165015.

Koley D, Bard AJ. Triton X-100 concentration effects on membrane permeability of a single HeLa cell by scanning electrochemical microscopy (SECM). Proc Natl Acad Sci USA 2010;107:16783–16787.

Koo H, Allan RN, Howlin RP, Stoodley P, Hall-Stoodley L. Targeting microbial biofilms: Current and prospective therapeutic strategies. Nat Rev Microbiol 2017;15:740–755.

Kooiman K, Vos HJ, Versluis M, de Jong N. Acoustic behavior of microbubbles and implications for drug delivery. Adv Drug Deliv Rev 2014;72:28–48.

Kripfgans OD, Fowlkes JB, Miller DL, Eldevik OP, Carson PL. Acoustic droplet vaporization for therapeutic and diagnostic applications. Ultrasound Med Biol 2000;26:1177–1189.

Kwan JJ, Myers R, Coviello CM, Graham SM, Shah AR, Stride E, Carlisle RC, Coussios CC. Ultrasound-propelled nanocups for drug delivery. Small 2015;11:5305–5314.

Kysela DT, Randich AM, Caccamo PD, Brun YV. Diversity takes shape: Understanding the mechanistic and adaptive basis of bacterial morphology. PloS Biol 2016;14 e1002565.

Lanjouw E, Ouburg S, de Vries H, Stary A, Radcliffe K, Unemo M. 2015 European guideline on the management of *Chlamydia trachomatis* infections. Int J STD AIDS 2016;27:333–348.

Lattwein KR, Shekhar H, van Wamel WJB, Gonzalez T, Herr AB, Holland CK, Kooiman K. An in vitro proof-of-principle study of sonobactericide. Sci Rep 2018;8:3411.

Lebeaux D, Ghigo JM, Beloin C. Biofilm-related infections: Bridging the gap between clinical management and fundamental aspects of recalcitrance toward antibiotics. Microbiol Mol Biol Rev 2014;78:510–543.

Lee SW, Gu H, Kilberg JB, Ren D. Sensitizing bacterial cells to antibiotics by shape recovery triggered biofilm dispersion. Acta Biomaterialia 2018;81:93–102.

Leighton TG. The acoustic bubble. London: Academic Press; 1994.

Lewis K. Persister cells and the riddle of biofilm survival. Biochem (Mosc) 2005;70:267–274.

Lewis K. Platforms for antibiotic discovery. Nat Rev Drug Discov 2013;12:371.

Li S, Zhu C, Fang S, Zhang W, He N, Xu W, Kong R, Shang X. Ultrasound microbubbles enhance human beta-defensin 3 against biofilms. J Surg Res 2015;199:458–469.

Liao AH, Hung CR, Lin CF, Lin YC, Chen HK. Treatment effects of lysozyme-shelled microbubbles and ultrasound in inflammatory skin disease. Sci Rep 2017;7:41325.

Liao X, Li J, Suo Y, Chen S, Ye X, Liu D, Ding T. Multiple action sites of ultrasound on *Escherichia coli* and *Staphylococcus* aureus. Food Sci Hum Wellness 2018;7:102–109.

Lin CY, Pitt WG. Acoustic droplet vaporization in biology and medicine. Biomed Res Int 2013;2013 404361.

Lin T, Cai XZ, Shi MM, Ying ZM, Hu B, Zhou CH, Wang W, Shi ZL, Yan SG. In vitro and in vivo evaluation of vancomycin-loaded PMMA cement in combination with ultrasound and microbubbles-mediated ultrasound. Biomed Res Int 2015;2015 309739.

Liu P, Wang X, Zhou S, Hua X, Liu Z, Gao Y. Effects of a novel ultrasound contrast agent with long persistence on right ventricular pressure: Comparison with SonoVue. Ultrasonics 2011;51:210–214.

Madsen HH, Rasmussen F. Contrast-enhanced ultrasound in oncology. Cancer Imaging 2011;11(Spec No A):S167–S173.

Magana M, Sereti C, Ioannidis A, Mitchell CA, Ball AR, Magiorkinis E, Chatzipanagiotou S, Hamblin MR, Hadjifrangiskou M, Tegos GP. Options and limitations in clinical investigation of bacterial biofilms. Clin Microbiol Rev 2018;31:e00084.

Mahalingam S, Xu Z, Edirisinghe M. Antibacterial activity and biosensing of PVA-lysozyme microbubbles formed by pressurized gyration. Langmuir 2015;31:9771–9780.

Mai-Prochnow A, Clauson M, Hong J, Murphy AB. Gram positive and Gram negative bacteria differ in their sensitivity to cold plasma. Sci Rep 2016;6:38610.

Malone M, Goeres DM, Gosbell I, Vickery K, Jensen S, Stoodley P. Approaches to biofilm-associated infections: The need for standardized and relevant biofilm methods for clinical applications. Expert Rev Anti-infect Ther 2017;15:147–156.

Mandell LA, Marrie TJ, Grossman RF, Chow AW, Hyland RH, Group at CC-APW. Canadian guidelines for the initial management of community-acquired pneumonia: An evidence-based update by the Canadian Infectious Diseases Society and the Canadian Thoracic Society. The Canadian Community-Acquired Pneumonia Working Group. Clin Infect Dis 2000;31:383–421.

Mannaris C, Averkiou MA. Investigation of microbubble response to long pulses used in ultrasound-enhanced drug delivery. Ultrasound Med Biol 2012;38:681–691.

Marks LR, Davidson BA, Knight PR, Hakansson AP. Interkingdom signaling induces *Streptococcus pneumoniae* biofilm dispersion and transition from asymptomatic colonization to disease. MBio 2013;4:e00438.

Maurice NM, Bedi B, Sadikot RT. *Pseudomonas aeruginosa* biofilms: Host response and clinical implications in lung infections. Am J Respir Cell Mol Biol 2018;58:428–439.

Mayer S, Grayburn PA. Myocardial contrast agents: Recent advances and future directions. Prog Cardiovasc Dis 2001;44:33–44.

McConoughey SJ, Howlin R, Granger JF, Manring MM, Calhoun JH, Shirtliff M, Kathju S, Stoodley P. Biofilms in periprosthetic orthopedic infections. Future Microbiol 2014;9:987–1007.

Menozzi G, Maccabruni V, Gabbi E. Left kidney infarction in a patient with native aortic valve infective endocarditis: Diagnosis with contrast-enhanced ultrasound. J Ultrasound 2013;16:145–146.

Menozzi G, Maccabruni V, Gabbi E, Leone N, Calzolari M. Contrast-enhanced ultrasound evaluation of splenic embolization in patients with definite left-sided infective endocarditis. Ultrasound Med Biol 2013;39:2205–2210.

Mermel LA, Allon M, Bouza E, Craven DE, Flynn P, O'Grady NP, Raad II, Rijnders BJA, Sherertz RJ, Warren DK. Clinical practice guidelines for the diagnosis and management of intravascular catheter-related infection: 2009 update by the Infectious Diseases Society of America. Clin Infect Dis 2009;49:1–45.

Miller RM, Zhang X, Maxwell AD, Cain CA, Xu Z. Bubble-induced color Doppler feedback for histotripsy tissue fractionation. IEEE Trans Ultrason Ferroelectr Freq Control 2016;63:408–419.

Moran CM, Watson RJ, Fox KA, McDicken WN. In vitro acoustic characterisation of four intravenous ultrasonic contrast agents at 30 MHz. Ultrasound Med Biol 2002;28:785–791.

Nishikawa T, Yoshida A, Khanal A, Habu M, Yoshioka I, Toyoshima K, Takehara T, Nishihara T, Tachibana K, Tominaga K. A study of the efficacy of ultrasonic waves in removing biofilms. Gerodontology 2010;27:199–206.

Nolsoe CP, Lorentzen T. International guidelines for contrast-enhanced ultrasonography: Ultrasound imaging in the new millennium. Ultrasonography 2016;35:89–103.

Nyborg WL. Acoustic streaming due to attenuated plane waves. J Acoust Soc Am 1953;25:68–75.

Oberbach A, Schlichting N, Feder S, Lehmann S, Kullnick Y, Buschmann T, Blumert C, Horn F, Neuhaus J, Neujahr R, Bagaev E, Hagl C, Pichlmaier M, Rodloff AC, Graber S, Kirsch K, Sandri M, Kumbhari V, Behzadi A, Behzadi A, Correia JC, Mohr FW, Friedrich M. New insights into valve-related intramural and intracellular bacterial diversity in infective endocarditis. PloS One 2017;12 e0175569.

Odekerken JCE, Logister DMW, Assabre L, Arts JJC, Walenkamp GHIM, Welting TJM. ELISA-based detection of gentamicin and vancomycin in protein-containing samples. SpringerPlus 2015;4:614.

Ohl SW, Klaseboer E, Khoo BC. Bubbles with shock waves and ultrasound: A review. Interface Focus 2015;5 20150019.

Okshevsky M, Meyer RL. Evaluation of fluorescent stains for visualizing extracellular DNA in biofilms. J Microbiol Methods 2014;105: 102–104.

Olson ME, Ceri H, Morck DW, Buret AG, Read RR. Biofilm bacteria: Formation and comparative susceptibility to antibiotics. Can J Vet Res 2002;66:86–92.

O'Reilly MA, Huang Y, Hynynen K. The impact of standing wave effects on transcranial focused ultrasound disruption of the blood-brain barrier in a rat model. Phys Med Biol 2010;55:5251–5267.

Osmon DR, Berbari EF, Berendt AR, Lew D, Zimmerli W, Steckelberg JM, Rao N, Hanssen A, Wilson WR. Diagnosis and management of prosthetic joint infection: Clinical practice guidelines by the iInfectious Diseases Society of America. Clin Infect Dis 2012;56:e1–e25.

Otto M. Staphylococcal biofilms. Curr Top Microbiol Immunol 2008;322:207–228.

Overvelde M, Garbin V, Dollet B, de Jong N, Lohse D, Versluis M. Dynamics of coated microbubbles adherent to a wall. Ultrasound Med Biol 2011;37:1500–1508.

Owens CA. Ultrasound-enhanced thrombolysis: EKOS endowave infusion catheter system. Semin Intervent Radiol 2008;25:37–41.

Parini MR, Pitt WG. Dynamic removal of oral biofilms by bubbles. Colloids Surf B Biointerfaces 2006;52:39–46.

Pitt WG, McBride MO, Lunceford JK, Roper RJ, Sagers RD. Ultrasonic enhancement of antibiotic action on gram-negative bacteria. Antimicrob Agents Chemother 1994;38:2577–2582.

Postema M, Bouakaz A, Chien Ting C, Jong ND. Optically observed microbubble coalescence and collapse. Proc IEEE Int Ultrason Symp 2002;2:1949–1952.

Qi X, Zhao Y, Zhang J, Han D, Chen C, Huang Y, Chen X, Zhang X, Wang T, Li X. Increased effects of extracorporeal shock waves combined with gentamicin against *Staphylococcus aureus* biofilms in vitro and in vivo. Ultrasound Med Biol 2016;42:2245–2252.

Roberts AEL, Kragh KN, Bjarnsholt T, Diggle SP. The limitations of in vitro experimentation in understanding biofilms and chronic infection. J Mol Biol 2015;427:3646–3661.

Ronan E, Edjiu N, Kroukamp O, Wolfaardt G, Karshafian R. USMB-induced synergistic enhancement of aminoglycoside antibiotics in biofilms. Ultrasonics 2016;69:182–190.

Rosenthal I, Sostaric JZ, Riesz P. Sonodynamic therapy—-A review of the synergistic effects of drugs and ultrasound. Ultrason Sonochem 2004;11:349–363.

Schneider M, Arditi M, Barrau MB, Brochot J, Broillet A, Ventrone R, Yan F. BR1: A new ultrasonographic contrast agent based on sulfur hexafluoride-filled microbubbles. Invest Radiol 1995;30:451–457.

Schneider M, Anantharam B, Arditi M, Bokor D, Broillet A, Bussat P, Fouillet X, Frinking P, Tardy I, Terrettaz J, Senior R, Tranquart F. BR38, a new ultrasound blood pool agent. Invest Radiol 2011;46:486–494.

Sharma PK, Gibcus MJ, van der Mei HC, Busscher HJ. Influence of fluid shear and microbubbles on bacterial detachment from a surface. Appl Environ Microbiol 2005;71:3668–3673.

Shen Y, Stojicic S, Qian W, Olsen I, Haapasalo M. The synergistic antimicrobial effect by mechanical agitation and two chlorhexidine preparations on biofilm bacteria. J Endod 2010;36:100–104.

Shi WT, Forsberg F, Tornes A, Østensen J, Goldberg BB. Destruction of contrast microbubbles and the association with inertial cavitation. Ultrasound Med Biol 2000;26:1009–1019.

Shi A, Min Y, Wan M. Flowing microbubble manipulation in blood vessel phantom using ultrasonic standing wave with stepwise frequency. Appl Phys Lett 2013;103 174105.

Short FL, Murdoch SL, Ryan RP. Polybacterial human disease: The ills of social networking. Trends Microbiol 2014;22:508–516.

Silhavy TJ, Kahne D, Walker S. The bacterial cell envelope. Cold Spring Harb Perspect Biol 2010;2 a000414.

Smeenge M, Tranquart F, Mannaerts CK, de Reijke TM, van de Vijver MJ, Laguna MP, Pochon S, de la Rosette JJMCH, Wijkstra H. First-in-human ultrasound molecular imaging with a VEGFR2-specific ultrasound molecular contrast agent (BR55) in prostate cancer: A safety and feasibility pilot study. Invest Radiol 2017;52:419–427.

Song KH, Fan AC, Hinkle JJ, Newman J, Borden MA, Harvey BK. Microbubble gas volume: A unifying dose parameter in blood-brain barrier opening by focused ultrasound. Theranostics 2017;7:144–152.

Sontum PC. Physicochemical characteristics of Sonazoid, a new contrast agent for ultrasound imaging. Ultrasound Med Biol 2008;34: 824–833.

Stewart PS, Costerton J. Antibiotic resistance of bacteria in biofilms. Lancet 2001;358:135–138.

Sugiyama MG, Mintsopoulos V, Raheel H, Goldenberg NM, Batt JE, Brochard L, Kuebler WM, Leong-Poi H, Karshafian R, Lee WL. Lung ultrasound and microbubbles enhance aminoglycoside efficacy and delivery to the lung in *Escherichia coli*–induced pneumonia and acute respiratory distress syndrome. Am J Respir Crit Care Med 2018;198:404–408.

Sun T, Zhang Y, Power C, Alexander PM, Sutton JT, Aryal M, Vykhodtseva N, Miller EL, McDannold NJ. Closed-loop control of targeted ultrasound drug delivery across the blood-brain/tumor barriers in a rat glioma model. Proc Natl Acad Sci USA 2017;114: E10281–E10290.

Sutton JT, Haworth KJ, Pyne-Geithman G, Holland CK. Ultrasound-mediated drug delivery for cardiovascular disease. Expert Opin Drug Deliv 2013;10:573–592.

Tandiono T, Ow DS, Driessen L, Chin CS, Klaseboer E, Choo AB, Ohl SW, Ohl CD. Sonolysis of *Escherichia coli* and *Pichia pastoris* in microfluidics. Lab Chip 2012;12:780–786.

ter Haar G. Safety and bio-effects of ultrasound contrast agents. Med Biol Eng Comput 2009;47:893–900.

ter Haar G. Ultrasound bioeffects and safety. Proc Inst Mech Eng H: J Eng Med 2010;224:363–373.

ter Haar G, Shaw A, Pye S, Ward B, Bottomley F, Nolan R, Coady A-M. Guidance on reporting ultrasound exposure conditions for bio-effects studies. Ultrasound Med Biol 2011;37:177–183.

Thomen P, Robert J, Monmeyran A, Bitbol A-F, Douarche C, Henry N. Bacterial biofilm under flow: First a physical struggle to stay, then a matter of breathing. PloS One 2017;12 e0175197.

Vakil N, Everbach EC. Transient acoustic cavitation in gallstone fragmentation: A study of gallstones fragmented in vivo. Ultrasound Med Biol 1993;19:331–342.

van Oosten M, Hahn M, Crane LMA, Pleijhuis RG, Francis KP, van Dijl JM, van Dam GM. Targeted imaging of bacterial infections: Advances, hurdles and hopes. FEMS Microbiol Rev 2015;39: 892–916.

van Rooij T, Daeichin V, Skachkov I, de Jong N, Kooiman K. Targeted ultrasound contrast agents for ultrasound molecular imaging and therapy. Int J Hyperthermia 2015;31:90–106.

van Rooij T, Beekers I, Lattwein KR, van der Steen AFW, de Jong N, Kooiman K. Vibrational responses of bound and nonbound targeted lipid-coated single microbubbles. IEEE Trans Ultrason Ferroelectr Freq Control 2017;64:785–797.

Vlaisavljevich E, Durmaz YY, Maxwell A, Elsayed M, Xu Z. Nanodroplet-mediated histotripsy for image-guided targeted ultrasound cell ablation. Theranostics 2013;3:851–864.

Vollmer AC, Kwakye S, Halpern M, Everbach EC. Bacterial stress responses to 1-megahertz pulsed ultrasound in the presence of microbubbles. Appl Environ Microbiol 1998;64:3927–3931.

Vyas N, Manmi K, Wang Q, Jadhav AJ, Barigou M, Sammons RL, Kuehne SA, Walmsley AD. Which parameters affect biofilm removal with acoustic cavitation? A review. Ultrasound Med Biol 2019;45:1044–1055.

Wang S, Hossack JA, Klibanov AL. Targeting of microbubbles: Contrast agents for ultrasound molecular imaging. J Drug Target 2018a;26: 420–434.

Wang M, Zhang Y, Cai C, Tu J, Guo X, Zhang D. Sonoporation-induced cell membrane permeabilization and cytoskeleton disassembly at varied acoustic and microbubble-cell parameters. Sci Rep 201b;8 Article 3885.

Ward M, Wu J, Chiu JF. Experimental study of the effects of Optison concentration on sonoporation in vitro. Ultrasound Med Biol 2000;26:1169–1175.

Wei K. Contrast echocardiography: Applications and limitations. Cardiol Rev 2012;20:25–32.

Werdan K, Dietz S, Loffler B, Niemann S, Bushnaq H, Silber RE, Peters G, Muller-Werdan U. Mechanisms of infective endocarditis: Pathogen−host interaction and risk states. Nat Rev Cardiol 2014;11:35–50.

Whiteley M, Diggle SP, Greenberg EP. Progress in and promise of bacterial quorum sensing research. Nature 2017;551:313–320.

Willmann JK, Bonomo L, Carla Testa A, Rinaldi P, Rindi G, Valluru KS, Petrone G, Martini M, Lutz AM, Gambhir SS. Ultrasound molecular imaging with BR55 in patients with breast and ovarian lesions: First-in-human results. J Clin Oncol 2017;35:2133–2140.

Xu J, Bigelow TA, Halverson LJ, Middendorf JM, Rusk B. Minimization of treatment time for in vitro 1.1 MHz destruction of *Pseudomonas aeruginosa* biofilms by high-intensity focused ultrasound. Ultrasonics 2012;52:668–675.

Yi S, Han G, Shang Y, Liu C, Cui D, Yu S, Liao B, Ao X, Li G, Li L. Microbubble-mediated ultrasound promotes accumulation of bone marrow mesenchymal stem cell to the prostate for treating chronic bacterial prostatitis in rats. Sci Rep 2016;6:19745.

Yu L, Zhong M, Wei Y. Direct fluorescence polarization assay for the detection of glycopeptide antibiotics. Anal Chem 2010;82: 7044–7048.

Zapotoczna M, O'Neill E, O'Gara JP. Untangling the diverse and redundant mechanisms of Staphylococcus aureus biofilm formation. PLoS Pathog 2016;12 e1005671.

Zhou M, Cavalieri F, Ashokkumar M. Modification of the size distribution of lysozyme microbubbles using a post-sonication technique. Instrum Sci Technol 2012;40:51–60.

Zhou H, Fang S, Kong R, Zhang W, Wu K, Xia R, Shang X, Zhu C. Effect of low frequency ultrasound plus fluorescent composite carrier in the diagnosis and treatment of methicillin-resistant *Staphylococcus aureus* biofilm infection of bone joint implant. Int J Clin Exp Med 2018;11:799–805.

Zhu C, He N, Cheng T, Tan H, Guo Y, Chen D, Cheng M, Yang Z, Zhang X. Ultrasound-targeted microbubble destruction enhances human beta-defensin 3 activity against antibiotic-resistant *Staphylococcus* biofilms. Inflammation 2013;36:983–996.

Zhu HX, Cai XZ, Shi ZL, Hu B, Yan SG. Microbubble-mediated ultrasound enhances the lethal effect of gentamicin on planktonic *Escherichia coli*. Biomed Res Int 2014;2014 142168.